Oxygen isotope fractionation during N_2O production by soil denitrification

D. Lewicka-Szczebak[1], J. Dyckmans[3], J. Kaiser[2], A. Marca[2], J. Augustin[4], R. Well[1]

[1]Thünen Institute of Climate-Smart Agriculture, Federal Research Institute for Rural Areas, Forestry and Fisheries, Bundesallee 50, 38116 Braunschweig, Germany

[2]Centre for Ocean and Atmospheric Sciences, School of Environmental Sciences, University of East Anglia, Norwich, NR4 7TJ, United Kingdom

[3]Centre for Stable Isotope Research and Analysis, University of Göttingen, Büsgenweg 2, 37077 Göttingen, Germany

[4]Leibniz Centre for Agricultural Landscape Research, Eberswalder Straße 84, 15374 Müncheberg, Germany

Correspondence to: D. Lewicka-Szczebak (dominika.lewicka@ti.bund.de)

Abstract

The isotopic composition of soil-derived N_2O can help differentiate between N_2O production pathways and estimate the fraction of N_2O reduced to N_2. Until now, $\delta^{18}O$ of N_2O has been rarely used in the interpretation of N_2O isotopic signatures because of the rather complex oxygen isotope fractionations during N_2O production by denitrification. The latter process involves nitrate reduction mediated through the following three enzymes: nitrate reductase (NAR), nitrite reductase (NIR) and nitric oxide reductase (NOR). Each step removes one oxygen atom as water (H_2O), which gives rise to a branching isotope effect. Moreover, denitrification intermediates may partially or fully exchange oxygen isotopes with ambient water, which is associated with an exchange isotope effect. The main objective of this study was to decipher the mechanism of oxygen isotope fractionation during N_2O production by soil denitrification and, in particular, to investigate the relationship between the extent of oxygen isotope exchange with soil water and the $\delta^{18}O$ values of the produced N_2O.

In our soil incubation experiments $\Delta^{17}O$ isotope tracing was applied for the first time to simultaneously determine the extent of oxygen isotope exchange and any associated oxygen isotope effect. We found that N_2O formation in static anoxic incubation experiments was typically associated with oxygen isotope exchange close to 100 % and a stable difference between the $^{18}O/^{16}O$ ratio of soil water and the N_2O product of $\delta^{18}O(N_2O/H_2O)$ = (17.5±1.2) ‰. However, flow-through experiments gave lower oxygen isotope exchange down to 56 % and a higher $\delta^{18}O(N_2O/H_2O)$ of up to 37 ‰. The extent of isotope exchange and $\delta^{18}O(N_2O/H_2O)$ showed a significant correlation (R^2 = 0.70, p < 0.00001). We hypothesise that this observation was due to the contribution of N_2O from another production process, most probably fungal denitrification.

An oxygen isotope fractionation model was used to test various scenarios with different magnitudes of branching isotope effects at different steps in the reduction process. The results suggest that during denitrification, isotope exchange occurs prior to isotope branching and that this exchange is mostly associated with the enzymatic nitrite reduction mediated by NIR. For bacterial denitrification, the branching isotope effect can be surprisingly low, about (0.0±0.9) ‰; in contrast to fungal denitrification where higher values of up to 30 ‰ have been reported previously. This suggests that $\delta^{18}O$ might be used as a tracer for differentiation between bacterial and fungal denitrification, due to their different magnitudes of branching isotope effects.

1. Introduction

Our ability to mitigate soil N_2O emissions is limited due to poor understanding of the complex interplay between N_2O production pathways in soil environments. In order to develop effective fertilizing strategies and reduce the loss of nitrogen through microbial consumption as well as related adverse environmental impacts (IPCC, 2013; Ravishankara et al., 2009), it is very important to fill the existing knowledge gaps. Isotopocule analyses of N_2O, including $\delta^{18}O$, average $\delta^{15}N$ ($\delta^{15}N^{av}$) and ^{15}N site preference within the linear N_2O molecule ($\delta^{15}N^{sp}$) have been used for several years to help differentiate between N_2O production pathways (Opdyke et al., 2009; Perez et al., 2006; Sutka et al., 2006; Toyoda et al., 2005; Well et al., 2008), the various microbes involved (Rohe et al., 2014a; Sutka et al., 2008; Sutka et al., 2003) and to estimate the fraction of N_2O reduced to N_2 (Ostrom et al., 2007; Park et al., 2011; Toyoda et al., 2011; Well and Flessa, 2009). However, the usefulness of these analyses would be enhanced further if the isotope fractionation mechanisms were better understood. In particular, we need to recognize the isotope effects associated with nitrate and N_2O reduction to quantify the entire gaseous nitrogen losses as N_2O and N_2 based on the N_2O isotopic signatures (Lewicka-Szczebak et al., 2015; Lewicka-Szczebak et al., 2014). This would be most effective if either of the isotopic signatures ($\delta^{18}O$, $\delta^{15}N^{av}$ or $\delta^{15}N^{sp}$) were stable or predictable for N_2O produced by each of the relevant N_2O forming processes (*e.g.* heterotrophic bacterial denitrification, fungal denitrification, nitrifier denitrification and nitrification). We hypothesize that this could be the case for $\delta^{18}O$, and this study aims to increase the understanding of the factors controlling $\delta^{18}O$ during N_2O production in soils. .

$\delta^{18}O(N_2O)$ has been rarely applied in the interpretation of N_2O isotopic signatures because of the rather complex oxygen isotope fractionations during N_2O production by denitrification (Kool et al., 2007). Denitrification is a stepwise process of nitrate reduction mediated by three enzymes: nitrate reductase (NAR), nitrite reductase (NIR) and nitric oxide reductase (NOR) (Fig. 1). $\delta^{18}O(N_2O)$ is controlled by the origin of the oxygen atom in the N_2O molecule (nitrate, nitrite, soil water or molecular O_2) and by the isotope fractionation during nitrate reduction or during oxygen isotope exchange with soil water.

[Fig. 1]

During each reduction step, one oxygen atom is detached and removed as water (H_2O), which is associated with branching isotope effects (Casciotti et al., 2007; Snider et al., 2013). Conceptually, these can be regarded as a combination of two isotope fractionations with opposite effects on the $\delta^{18}O$ signature of the reduction product: (i) intermolecular fractionation due to preferential reduction of ^{18}O-depleted molecules, which results in ^{18}O-enriched residual substrate and ^{18}O-depleted product, and (ii) intramolecular fractionation due to preferential ^{16}O abstraction, which results in ^{18}O-enriched nitrogen-bearing reduction products and ^{18}O-depleted H_2O as side product. Since intermolecular fractionation causes ^{18}O depletion of the reduction product and intramolecular fractionation causes ^{18}O enrichment, the net branching effect (ε_n), as the sum of both, can theoretically vary between negative and positive values. However, pure cultures studies show that ε_n is mostly positive, *i.e.* between 25 and 30 ‰ for bacterial denitrification (Casciotti et al., 2007) and between 10 and 30 ‰ for fungal denitrification (Rohe et al., 2014a). Importantly, the intra- and intermolecular isotope effects can only manifest together during incomplete substrate consumption (Rohe et al., 2014a). In case of complete substrate conversion, the net branching effect reflects the intramolecular effect only (Casciotti et al., 2007).

Moreover, denitrification intermediates may partially or fully exchange oxygen isotopes with ambient water (Kool et al., 2009). The isotopic signature of the incorporated O-atom depends on the isotopic signature of ambient water and the isotope fractionation associated with this exchange. Under typical soil conditions, *i.e.* pH close to neutral and moderate temperatures, abiotic isotope exchange between nitrate and water is negligibly slow. In extremely acid conditions (pH < 0), the equilibrium effect is $\varepsilon(NO_3^-/H_2O)$ = 23 ‰ (Böhlke et al., 2003). Casciotti et al. (2007) showed that for nitrite the abiotic exchange can occur at neutral pH, but for achieving an isotopic equilibrium over 8 months are needed. The observed isotope equilibrium effect between nitrite and water is $\varepsilon(NO_2^-/H_2O)$ = 14 ‰ at 21 ºC. Nothing is known yet about the possible abiotic exchange between NO and ambient water. The isotope exchange between denitrification intermediates and ambient water is most probably accelerated by enzymatic catalysis, since numerous ^{18}O tracer studies documented nearly complete O isotope exchange (Kool et al., 2009; Rohe et al., 2014b; Snider et al., 2013) within short incubation times like a few hours. Hence, it can be assumed that at least one enzymatic step must be responsible for exchange of O isotopes with soil water (Rohe et al., 2014a; Snider et al., 2013). In pure culture studies the extent of oxygen isotope exchange ranged from 4 to 100 % for bacterial denitrification (Kool et al., 2007) and from 11 to 100 %

for fungal denitrification (Rohe et al., 2014b). In contrast, unsaturated soil incubation experiments, with a natural whole microbial community, showed consistently high magnitudes of oxygen isotope exchange between 85 and 99 % (Kool et al., 2009; Lewicka-Szczebak et al., 2014; Snider et al., 2013). If the high extent of isotope exchange was characteristic of soil denitrification processes, we would expect quite stable $\delta^{18}O$ values of the produced N_2O during denitrification.

It is difficult to quantitatively link isotope exchange and apparent isotope effects, because using the ^{18}O tracer technique to quantify isotope exchange prevents simultaneous study of isotope oxygen fractionation. However, two studies that conducted parallel ^{18}O traced and natural abundance experiments allowed formulating general oxygen isotope fractionation models (Rohe et al., 2014a; Snider et al., 2013). These models showed that the magnitude of overall isotope fractionation depends not only on the extent of oxygen isotope exchange but also on the enzymatic reduction step associated with this exchange (Fig. 1). It was found that the oxygen isotope exchange is predominantly associated with NIR for fungal denitrification (Rohe et al., 2014a). Fungi and bacteria are characterized by different NOR mechanisms (Schmidt et al., 2004; Stein and Yung, 2003), resulting in distinct $\delta^{15}N^{sp}$ values for bacterial and fungal denitrification. It is possible that these different NOR mechanisms also influence $\delta^{18}O$.

In the present study, we used ^{17}O as tracer to determine the extent of O isotope exchange, in order to separate isotope exchange and apparent isotope effects. We applied a nitrate fertilizer of natural atmospheric deposition origin with high ^{17}O excess, as a result of non-random oxygen isotope distribution. Then we measured ^{17}O excess of the produced N_2O and, based on the observed loss of ^{17}O excess, calculated the extent of isotope exchange with water. Simultaneously, we could measure the $^{18}O/^{16}O$ fractionation in the same incubation vessels, since the ^{17}O tracing method has no impact on $\delta^{18}O$. This is the first time that such an approach has been used. To validate this method, we applied an alternative approach, namely, soil water with distinct $\delta^{18}O$ values within the range of natural abundance isotopic signatures was applied to quantify isotope exchange (Snider et al., 2009). The latter method has also been applied in a recent soil incubation study (Lewicka-Szczebak et al., 2014) and indicated almost complete oxygen isotope exchange with soil water associated with a stable isotope ratio difference between soil water and produced N_2O of $\delta^{18}O(N_2O/H_2O)$ = (19.0±0.7) ‰. However, the results of other experiments presented in the same study (Lewicka-Szczebak et

al., 2014) indicated much higher $\delta^{18}O(N_2O/H_2O)$ values of up to 42 ‰. The higher values may be due to a lower extent of oxygen isotope exchange, but no data were available regarding the extent of exchange for those samples. In the present study, we investigated possible controlling factors for oxygen isotope exchange by applying various experimental treatments differing in soil moisture and temperature.

The combination of various experimental approaches allowed us to further improve the $\delta^{18}O$ fractionation model proposed by Snider et al. (2013) and Rohe et al. (2014a), to decipher the mechanism of oxygen isotope fractionation during N_2O production by denitrification and to determine the associated isotope effects. We investigated the variability of isotope exchange with soil water and of the $\delta^{18}O$ values of produced N_2O under varying conditions as well as the relation between these quantities. Ultimately, our aim was to check to what level of accuracy $\delta^{18}O$ can be predicted based on the known controlling factors.

Additionally, the ^{17}O analyses of N_2O produced by denitrification gave us the opportunity to test the hypothesis of soil denitrification contributing to the non-random distribution of oxygen isotopes (^{17}O excess, or $\Delta^{17}O$) in atmospheric N_2O (Kaiser et al., 2004; Michalski et al., 2003).

2. Methods

2.1. Experimental set-ups

2.1.1. Experiment 1 (Exp 1) – static anoxic incubation

The static incubations were performed under an anoxic atmosphere (N_2) in closed, gas-tight vessels where denitrification products accumulated in the headspace. Two arable soil types were used: a *Luvisol* with loamy sand texture and *Haplic Luvisol* with silt loam texture with pH (in 0.01 M $CaCl_2$) of 5.7 and 7.4, respectively. More details on soil properties can be found in Lewicka-Szczebak et al. (2014). For the first part of these incubations (Exp 1.1) two different temperature treatments were applied (8 and 22 ºC) and only one moisture treatment of 80 % WFPS (water filled pore space). The results of $\delta^{18}O(N_2O)$ analyses for these samples have already been published (Lewicka-Szczebak et al., 2014). Here we expand these data with $\Delta^{17}O(N_2O)$ analyses. The second part of the static incubations (Exp 1.2) was performed for the same two soils with three different moisture treatments of 50, 65 and 80 % WFPS at one

temperature (22 ºC). Details on the treatments are presented as supplementary information in Table A1.

This experimental approach is described in detail in Lewicka-Szczebak et al. (2014). In short, the soil was air dried and sieved at 2 mm mesh size. Afterwards, the soil was rewetted to obtain the target WFPS and fertilised with 50 (Exp 1.1) or 10 (Exp 1.2) mg N equivalents (as $NaNO_3$) per kg soil. Various nitrate and water treatments were applied (Table A1). The soils were rewetted using two waters with distinct isotopic signatures: *heavy water* ($\delta^{18}O$ = -1.5 ‰) and *light water* ($\delta^{18}O$ = -14.8 ‰) and fertilized with two different nitrate fertilizers: natural *Chile saltpeter* ($NaNO_3$, Chili Borium Plus, Prills-Natural origin, supplied by Yara, Dülmen, Germany, $\delta^{18}O$ = 56 ‰) and *synthetic* $NaNO_3$ (Sigma Aldrich, Taufkirchen, Germany, $\delta^{18}O$ = 27 ‰). The soils were thoroughly mixed to obtain a homogenous distribution of water and fertilizer and an equivalent of 100 g of dry soil was repacked into each incubation jar at bulk densities of 1.3 g cm^{-3} for the silt loam soil and 1.6 g cm^{-3} for the loamy sand soil. The 0.8 dm^3 Weck jars (J. WECK GmbH u. Co. KG, Wehr, Germany) were used with airtight rubber seals and with two three-way valves installed in their glass cover to enable sampling and flushing. The jars were flushed with N_2 at approximately 500 cm^3 min^{-1} (STP: 273.15 K, 100 kPa) for 10 min to create anoxic conditions. Immediately after flushing, acetylene (C_2H_2) was added to inhibit N_2O reduction in selected jars (C_2H_2 inhibited treatment), by replacing 80 cm^3 of N_2 with C_2H_2, which resulted in 10 kPa C_2H_2 in the headspace. Each treatment (Table 1A) had three replicates. The soils were incubated for approximately 25 hours and three to four samples were collected at 4 to 12 hour-intervals by transferring 30 cm^3 of headspace gases into two pre-evacuated 12 cm^3 Exetainer vials (Labco Limited, Ceredigion, UK). The excess 3 cm^3 of headspace gas in each vial ensured that no ambient air entered the vials. The removed sample volume was immediately replaced by pure N_2 gas.

Additional treatments with addition of ^{15}N-labelled $NaNO_3$ (98 % ^{15}N isotopic purity) were used to control the efficiency of acetylene inhibition and to determine the N_2O mole fraction $f(N_2O) = c(N_2O)/[c(N_2)+c(N_2O)]$ (c: volumetric concentration) in non-inhibited treatments. This method allows determination of the N_2 concentration originating from the ^{15}N labelled pool and hence the N_2O mole fraction (Lewicka-Szczebak et al., 2013).

2.1.2. Experiment 2 (Exp 2) – flow-through incubation under He atmosphere

The flow-through incubations were performed using a special gas-tight incubation system allowing for incubation under N_2-free atmosphere to enable direct quantification of soil N_2 fluxes (Butterbach-Bahl et al., 2002; Scholefield et al., 1997). This system has been described in detail by Eickenscheidt et al. (2014). Four different soils were incubated: two arable soils, same as in Exp 1 (loamy sand and silt loam) and two grassland soils: an organic soil classified as *Histic Gleysol* and a sandy soil classified as *Plaggic Anthrosol*, with pH (in 0.01 M $CaCl_2$) of 5.9 and 5.3, respectively. All soils were incubated at the target moisture level of 80 % WFPS and the two most active soils (organic and silt loam soil) were additionally incubated at the lower moisture level of 70 % WFPS (target values, for actual values see Table 2).

The soils were air dried and sieved at 4 mm mesh size. Afterwards, the soil was rewetted to obtain 70 % WFPS and fertilised with 50 mg N equivalents (as $NaNO_3$) per kg soil with natural fertilizer *Chile saltpetre.* The soils were thoroughly mixed to obtain a homogenous distribution of water and fertilizer and 250 cm^3 of wet soil was repacked into each incubation vessel at bulk densities of 1.4 g cm^{-3} for the silt loam soil, 1.6 g cm^{-3} for the loamy sand soil, 1.5 g cm^{-3} for the sandy soil, and 0.4 g cm^{-3} for the organic soil. Afterwards, the water deficit to the target WFPS was added on the top of the soil for 80% WFPS treatments. Each treatment had three replicates. The incubation vessels were cooled to 2 ºC and repeatedly evacuated (to 4.7 kPa) and flushed with He to reduce the N_2 background and afterwards flushed with a continuous flow of 20 % O_2 in helium (He/O_2) mixture at 15 cm^3 min^{-1} (STP) for at least 60 hours. When a stable and low N_2 background (below 10 μmol mol^{-1}) was reached, temperature was increased to 22 ºC. During the incubation the headspace was constantly flushed with He/O_2 mixture (first 3 days; Part 1) and then with He (last 2 days; Part 2) at a flow rate of approximately 15 cm^3 min^{-1} (STP). The fluxes of N_2O and N_2 were analyzed immediately (see Sect. 2.2) and $f(N_2O)$ was determined. Samples for N_2O isotopocule analyses were collected by connecting the sampling vials in line with the exhaust gas of each incubation vessels and exchanging them at least twice a day. The results presented in this study originate from the anoxic Part 2 of the incubation, since the N_2O fluxes during the Part 1 were too low for $\Delta^{17}O$ analyses. The results for two samples taken approximately 8 and 24 h after switch to anoxic conditions are shown.

2.2. Gas chromatographic analyses

In Exp 1 the samples for gas concentration analyses were collected in Exetainer vials (Labco Limited, Ceredigion, UK) and were analysed using an Agilent 7890A gas chromatograph

(GC) (Agilent Technologies, Santa Clara, CA, USA) equipped with an electron capture detector (ECD). Measurement repeatability as given by the relative standard deviation (1σ) of four standard gas mixtures was typically 1.5 %.

In Exp 2, online trace gas concentration analysis of N_2 was performed with a micro-GC (Agilent Technologies, 3000 Micro GC), equipped with a thermal conductivity detector (TCD) and N_2O was measured with a GC (Shimadzu, Duisburg, Germany, GC–14B) equipped with ECD detector. The measurement repeatability (1σ) was better than 0.02 μmol mol^{-1} for N_2O and 0.2 μmol mol^{-1} for N_2.

2.3. Isotopic analyses

2.3.1. Isotopocules of N_2O

Gas samples were analyzed using a Delta V isotope ratio mass spectrometer (Thermo Scientific, Bremen, Germany) coupled to automatic preparation system: Precon + Trace GC Isolink (Thermo Scientific, Bremen, Germany) where N_2O was preconcentrated, separated and purified. In the mass spectrometer, N_2O isotopocule signatures were determined by measuring *m/z* 44, 45, and 46 of intact N_2O^+ ions as well as *m/z* 30 and 31 of NO^+ fragments ions. This allows the determination of average $\delta^{15}N^{av}$, $\delta^{15}N^{\alpha}$ ($\delta^{15}N$ of the central N position of the N_2O molecule), and $\delta^{18}O$ (Toyoda and Yoshida, 1999). $\delta^{15}N^{\beta}$ ($\delta^{15}N$ of the peripheral N position of the N_2O molecule) is calculated using $\delta^{15}N^{av} = (\delta^{15}N^{\alpha} + \delta^{15}N^{\beta}) / 2$. The ^{15}N site preference ($\delta^{15}N^{sp}$) is defined as $\delta^{15}N^{sp} = \delta^{15}N^{\alpha} - \delta^{15}N^{\beta}$. The scrambling factor and ^{17}O-correction were taken into account (Kaiser and Röckmann, 2008; Röckmann et al., 2003). Pure N_2O (Westfalen, Münster, Germany) was used as internal reference gas and was analyzed in the laboratory of the Tokyo Institute of Technology using calibration procedures reported previously (Toyoda and Yoshida, 1999; Westley et al., 2007). Moreover, the comparison materials from an intercalibration study (S1, S2) were used to perform a two-point calibration (Mohn et al., 2014). For correction of non-linear effect due to variable sample amount five different standard gas mole fractions (0.3, 1, 5, 10, 20 μmol mol^{-1}) were analyzed in each sample run. Samples with similar N_2O mole fractions were run together with at least two standard gases with similar mole fractions.

All isotopic signatures are expressed as relative deviation (in ‰) from the $^{15}N/^{14}N$, $^{17}O/^{16}O$ and $^{18}O/^{16}O$ ratios of the reference materials (*i.e.*, atmospheric N_2 and Vienna Standard Mean

Ocean Water (VSMOW), respectively). The measurement repeatability (1σ) of the internal standard (filled into vials and measured in the same way as the samples) for measurements of $\delta^{15}N^{av}$, $\delta^{18}O$ and $\delta^{15}N^{sp}$ was typically 0.1, 0.1, and 0.5 ‰, respectively.

2.3.2. $\delta^{18}O$ of NO_3^-

Soil nitrate was extracted in 0.01 M aqueous $CaCl_2$ solution (weight ratio soil:solution 1:10) by shaking at room temperature for one hour. $\delta^{18}O$ of nitrate in the soil solution was determined using the bacterial denitrification method (Casciotti et al., 2002). The measurement repeatability (1σ) of the international standards (USGS34, USGS35, IAEA-NO-3) was typically 0.5 ‰ for $\delta^{18}O$.

2.3.3. $\Delta^{17}O$ excess in N_2O and NO_3^-

N_2O samples collected from soil incubation and N_2O produced from soil NO_3^- by the bacterial denitrifier method were analysed for $\Delta^{17}O$ using the thermal decomposition method (Kaiser et al., 2007) with a gold oven (Exp 1.1b,c and 1.2a,b) and with a gold-wire oven (Exp 1.1a and 2) (Dyckmans et al., 2015) . The ^{17}O excess, $\Delta^{17}O$, is defined as (Kaiser et al., 2007):

$$\Delta^{17}O = \frac{1+\delta^{17}O}{(1+\delta^{18}O)^{0.5279}} - 1 \qquad (1)$$

The measurement repeatability (1σ) of the international standards (USGS34, USGS35) was typically 0.5 ‰ for $\Delta^{17}O$.

2.3.4. *Soil water analyses*

Soil water was extracted with the method described by Königer et al. (2011) and $\delta^{18}O$ of water samples (with respect to VSMOW) was measured using cavity ringdown spectrometer Picarro L1115-*i* (Picarro Inc., Santa Clara, USA). The measurement repeatability (1σ) of the internal standards (three calibrated waters with known $\delta^{18}O$: -19.67 ‰, -8.60 ‰, +1.37 ‰) was below 0.1 ‰. The overall error associated with the soil water extraction method determined as standard deviation (1σ) of the 5 samples replicates was below 0.5 ‰.

2.4. Determination of the extent of isotope exchange

The extent of isotope exchange (x) was determined with two independent methods described below. In Exp 1 both approaches were applied simultaneously on the same soil samples, which allowed quantifying the oxygen isotope exchange with two different methods independently. This enabled the validation of the ^{17}O excess method, which was used here for the first time for quantification of isotope exchange. Afterwards this validated method was applied in the following Exp 2. For both presented methods it is assumed that after N_2O is formed, no further oxygen isotope exchange with H_2O occurs.

2.4.1. $\delta^{18}O$ method

This method determines the isotope exchange based on the relative difference between $\delta^{18}O$ of produced N_2O and its potential precursors: soil water and soil nitrate (Snider et al., 2009). To make this method applicable, parallel incubations with distinct water and/or nitrate isotopic signatures must be carried out. Therefore, treatments with different water and nitrate isotopic signatures were applied in Exp. 1 (Table 1, Table A1). The calculation is based on two end member mixing model (water (δ_w) and nitrate (δ_n); δ stands for $\delta^{18}O(N_2O)$) taking into account the isotope fractionation associated with O atom incorporation into N_2O from each end member (ε_w - fractionation associated with oxygen isotope exchange with water, ε_n - fractionation associated with branching effect during nitrate reduction). This is expressed as:

$$1+\delta = x(1+\delta_w)(1+\varepsilon_w) + (1-x)(1+\delta_n)(1+\varepsilon_n) \quad (2)$$

which can be rearranged to:

$$\frac{\delta-\delta_n}{1+\delta_n} = x(1+\varepsilon_w)\frac{\delta_w-\delta_n}{1+\delta_n} + x\varepsilon_w + (1-x)\varepsilon_n \quad (3)$$

where:

$\frac{\delta-\delta_n}{1+\delta_n} = \delta^{18}O(N_2O/NO_3^-) =$ dependent variable of the linear regression

$\frac{\delta_w-\delta_n}{1+\delta_n} = \delta^{18}O(H_2O/NO_3^-) =$ independent variable of the linear regression

$x(1+\varepsilon_w) =$ slope of the linear regression ≅ the magnitude of isotope exchange (x)

$x\varepsilon_w + (1-x)\varepsilon_n =$ intercept of the linear regression ≅ total fractionation (ε)

Hence, from the linear correlation between $\delta^{18}O(N_2O/NO_3^-)$ and $\delta^{18}O(H_2O/NO_3^-)$ we can approximate x (the deviation from the exact value may be up to 0.02, for ε_w < 20 ‰) and the total fractionation ε comprised of both ε_w and ε_n.

2.4.2. $\Delta^{17}O$ method

This method determines the isotope exchange based on the comparison of $\Delta^{17}O$ in soil nitrate and produced N_2O. It requires the application of nitrate characterised by high $\Delta^{17}O$. Therefore, soils were amended with natural $NaNO_3$ *Chile saltpeter* showing high $\Delta^{17}O$ (ca. 20 ‰) and the $\Delta^{17}O$ of the N_2O product was measured. $\Delta^{17}O$ of soil water was assumed to be 0 ‰.

The magnitude of oxygen isotope exchange (x) was calculated as:

$$x = 1 - \frac{\Delta^{17}O(N_2O)}{\Delta^{17}O(NO_3^-)} \quad (4)$$

The error due to the use of the power-law definition of $\Delta^{17}O$ in combination with a linear mixing relationship (Eq. (4)) causes a negligible relative bias of <1 % for x.

2.5. Correction for N_2O reduction

Since $\delta^{18}O(N_2O)$ values of emitted N_2O are strongly affected by partial N_2O reduction, the measured isotope values can only be informative for the mechanism of N_2O production if the reduction is inhibited or the isotope effects associated with reduction are taken into account. Exp 1, where we applied both C_2H_2-inhibited as well as uninhibited treatments (Table 1), allows us to check the validity of our correction methods as it directly yields the impact of N_2O reduction on the measured $\delta^{18}O(N_2O)$ values. In Exp 2, reduction was not inhibited and the mathematical correction described below was applied.

The correction was made using the Rayleigh fractionation equation (Mariotti et al., 1981):

$$\frac{1+\delta_S}{1+\delta_{S0}} = f^{\varepsilon} \quad (5)$$

where: δ_S – isotopic signature of the remaining substrate, here: measured $\delta^{18}O$ of the final, partially reduced, N_2O, δ_{S0} – initial isotopic signature of the substrate, here: $\delta^{18}O$ of the produced N_2O unaffected by the reduction ($\delta_0{}^{18}O$); to be calculated; f – remaining unreacted fraction, here: the N_2O mole fraction $f(N_2O)$; directly measured; ε – isotope effect between

product and substrate, here: $\varepsilon(N_2/N_2O)$, the isotope effect associated with N_2O reduction, taken from the literature (Lewicka-Szczebak et al., 2014). As it has been shown that the experimental approach largely influences O isotope effect during reduction (Lewicka-Szczebak et al., 2015; Lewicka-Szczebak et al., 2014), we used different $\varepsilon^{18}O(N_2/N_2O)$ values for static and flow-through incubations. For the static Exp. 1 a mean $\varepsilon^{18}O(N_2/N_2O)$ value of -17.4 ‰ is used, based on one common experiment between the study of Lewicka-Szczebak et al. (2014) (Experiment 1) and this study (Exp 1.1). For the flow-through Exp 2 we accept the $\varepsilon^{18}O(N_2/N_2O)$ value of -12 ‰ recently determined for similar flow-through experiments under He/O_2 atmosphere (Lewicka-Szczebak et al., 2015). For the correction of $\delta^{15}N^{sp}$ values one common $\varepsilon^{15}N^{sp}(N_2/N_2O)$ value of -5 ‰ was used, since it was shown that this value is applicable for all experimental setups (Lewicka-Szczebak et al., 2014). The error due to the simplified use of $\varepsilon^{15}N^{sp}$ for the Rayleigh model (Eq. (5)) instead of separate calculations with $\varepsilon^{15}N^{\alpha}$ and $\varepsilon^{15}N^{\beta}$, causes a negligible bias of the calculated $\delta_0{}^{15}N^{sp}$ values of <0.15 ‰ for the presented dataset.

2.6. N_2O isotopic signatures related to water

Relative isotope ratio differences between N_2O and soil water, $\delta^{18}O(N_2O/H_2O)$, were calculated as the difference between the measured $\delta^{18}O$ of produced N_2O and of soil water:

$$\delta^{18}O(N_2O/H_2O) = \frac{\delta^{18}O(N_2O) - \delta^{18}O(H_2O)}{1 + \delta^{18}O(H_2O)} \quad (6)$$

In samples where N_2O reduction occurred $\delta^{18}O(N_2O/H_2O)$ values were corrected as described above (Sect. 2.5) and for statistical analyses and modelling exercises the reduction-corrected values were used ($\delta_0{}^{18}O(N_2O/H_2O)$).

2.7. Statistical methods

For results comparisons, ANOVA variance analysis was used with the significance level α of 0.05. The uncertainty values provided for the measured parameters represent the standard deviation (1σ) of the replicates. The propagated uncertainty was calculated using Gauss' error propagation equation taking into account standard deviations of all individual parameters.

3. Results & Discussion

3.1. Exp 1

In Table 1 the results are presented as average values from three replicated incubation vessels with respective standard deviation. Soil nitrate and water were analysed at the beginning of the experiment from the prepared homogenised soils, hence no standard deviation but the standard analytical uncertainty is given.

For different temperature treatments, x (determined by the $\Delta^{17}O$ method) was not significantly different (p = 0.19) but $\delta_0{}^{18}O(N_2O/H_2O)$ was slightly higher (p = 0.009) for 8 ºC ((19.5±0.3) ‰) than for 22 ºC ((18.6±0.3) ‰) treatment. No significant differences were observed between the two analysed soil types or between various soil moisture levels.

When comparing Exp 1.1 and 1.2, x did not show any significant differences, but the $\delta_0{}^{18}O(N_2O/H_2O)$ values were significantly different (p < 0.001) with higher values for Exp 1.1 ((19.1 ± 0.5) ‰) than for Exp 1.2 ((16.9 ± 0.8) ‰). It should be noted that the $\delta^{18}O$ values of soil nitrate were much lower in Exp 1.2 (from -2.0 to 6.5 ‰) when compared to Exp 1.1 (from 31.8 to 42.6 ‰) which might have affected the observed differences in $\delta_0{}^{18}O(N_2O/H_2O)$.

[Table 1]

Moreover, for Exp 1 the $\delta^{18}O$ method was applied to estimate x and ε from the relationship between $\delta^{18}O(N_2O/NO_3)$ and $\delta^{18}O(H_2O/NO_3)$ as described in 2.4.1.

[Fig. 2]

According to this method, from the linear regression one can decipher x (slope) and ε (intercept) (Snider et al., 2009). The correlation is excellent (R^2 from 0.989 to 0.997) which

indicates that the x and ε are very stable for all the treatments (Fig. 2). The x is about 1 (complete exchange) and ε varies from 17.1 (Exp 1.2) to 18.2 ‰ (Exp 1.1). When compared to the results presented in Table 1, we see slightly higher isotope exchange with $\delta^{18}O$ method when compared to $\Delta^{17}O$ method. This may be partially due to the fact that the slope in $\delta^{18}O$ method (Fig. 2) is actually slightly higher than x (from Eq. (3): $x(1+\varepsilon_w)$). The difference between the two experiments is mostly within the error of each method, so far the results are consistent. The $\Delta^{17}O$ method is more useful, since it allows for individual determinations of x, whereas the correlation obtained from the $\delta^{18}O$ method is based on all data, hence provides a mean result for x and ε for a whole experiment.

Importantly, we found that the $\delta^{18}O$ method is not applicable to samples with uninhibited N_2O reduction, if $\delta^{18}O(N_2O)$ values are not corrected for N_2O reduction. The treatment with uninhibited reduction of Exp 1.1 was tested and provided very different results, *i.e.* largely overestimated x (1.5) and ε (44.8) (red dashed fit line, Fig.2). Hence, for proper determination of these factors the results from treatments with inhibited N_2O reduction were used (solid black fit line, Fig.2). However, the $\delta^{18}O$ values after mathematical correction for N_2O reduction (red '+' points, Fig.2) fitted very well to the correlation found for inhibited samples. Hence, the reduction corrected values ($\delta_0{}^{18}O(N_2O)$) should rather be used when applying this method in experiments with uninhibited N_2O reduction. Moreover, in both static experiments we used the C_2H_2 inhibition technique, and our results indicate almost complete exchange of oxygen isotopes with soil water, which indicates that the isotope exchange process is not inhibited by C_2H_2 addition.

3.2. Exp 2

In Table 2 the results are presented as average values from three replicate incubation vessels with respective standard deviation. The extent of oxygen isotope exchange (x) ranges from 55 to 85 % and is lower and much more variable when compared to Exp 1. $\delta_0{}^{18}O(N_2O/H_2O)$ varies between 18.6 and 36.9 ‰, which is significantly higher when compared to the values determined in Exp 1.

[Table 2]

3.3. Oxygen isotope effects at nearly complete isotope exchange

In case of very high, almost complete, isotope exchange with soil water (Exp 1), the relative isotope ratio difference between N_2O and H_2O ($\delta_0{}^{18}O(N_2O/H_2O)$) is quite stable and ranges from 15.6 to 19.8 ‰ (Table 1). In contrast, the relative isotope ratio difference between N_2O and NO_3^- ($\delta_0{}^{18}O(N_2O/NO_3^-)$) shows large variations from -36.1 to 18.0 ‰ (Fig. 3).

[Fig. 3]

ε determined in Fig.2 represents theoretically the total oxygen isotope fractionation (from Eq. (3): $x\varepsilon_w + (1–x)\varepsilon_n$), but in case of the nearly whole isotope exchange ($x = 1$) ε equals ε_w and $\varepsilon_w = (\delta_{N2O}-\delta_w)/(\delta_w+1) = \delta^{18}O(N_2O/H_2O)$, hence both - the intercept in Fig. 2 and $\delta^{18}O(N_2O/H_2O)$ in Fig. 3 should provide rough estimates for ε_w. However, for x<1 $\delta^{18}O(N_2O/H_2O)$ depends also on δ_n and ε_n and the intercept (Fig.2) includes ε_n. Both these values indicate a slight difference between both experiments, for Exp 1.1 ε of (18.2±0.6) (intercept, Fig.2) and $\delta^{18}O(N_2O/H_2O)$ of (19.1±0.5) (mean±SD, Table 1) are higher than for Exp 1.2, (17.1±0.3) and (16.7±0.8), respectively. This slight difference is most probably due to *x* slightly lower than 1, as indicated by $\Delta^{17}O$ method and additional impact of δ_n and ε_n. It can be noted that $\delta_0{}^{18}O(N_2O/H_2O)$ slightly increases with higher $\delta^{18}O$ values of nitrate (Fig. 3), *i.e.* the difference of about 40 ‰ in $\delta^{18}O$ of applied NO_3^- results in about 2 ‰ change in $\delta_0{}^{18}O(N_2O/H_2O)$. Hence, only about 5 % of the difference in nitrate isotopic signature is reflected in the produced N_2O, suggesting that an equivalent percentage of $O(N_2O)$ originated from NO_3^-. This is very consistent with the determined extent of isotope exchange with soil water, which was (95.6±2.6) % (Table 1).

Taken together, the data indicates that the $\delta^{18}O(N_2O)$ values are clearly influenced by the $\delta^{18}O$ of soil water, whereas $\delta^{18}O$ of soil nitrates has only very little influence. Hence, the O isotope fractionation during N_2O production by denitrification should be considered in relation to soil water, rather than soil nitrates.

3.4. Oxygen isotope effects at variable isotope exchange

In contrast to Section 3.3, *x* was more variable for the flow-through incubation (Exp. 2) and also significantly lower. In general, lower *x* was associated with higher $\delta_0{}^{18}O(N_2O/H_2O)$ values. In Fig. 4 we can compare results from static incubations (red symbols) with the flow-through incubations (black symbols). This comparison clearly shows that the pattern of isotope exchange and associated oxygen fractionation differs significantly between both experimental approaches. The essential difference in Exp 2 was the use of a flow-through system with an oxic atmosphere at the beginning of the incubation (though results presented originate from the anoxic phase). This resulted in lower production rates for N_2O when comparing the respective soil (Table 1 and 2), *e.g.*, 80 μg kg^{-1} h^{-1} (mass of N as sum of N_2O and N_2 per mass of dry soil) for the silt loam soil at 80 % WFPS in Exp 2.3 but 261 μg kg^{-1} h^{-1} in Exp 1.1c. This may suggest an impact of N_2O production rate on extent of isotope exchange. However, for static anoxic incubations the effect of production rate was not observed, *e.g.* between 1.1a and 1.1b (Table 1), where we have different production rates but similar *x* and $\delta_0{}^{18}O(N_2O/H_2O)$.

[Fig. 4]

Interestingly, the correlation between *x* and $\delta_0{}^{18}O(N_2O/H_2O)$ seems to differ for different soil types. Very clearly both sandy soils represent distinct and weaker correlation when compared to silt loam and organic soil. Most probably this is due to different oxygen fractionation pattern during N_2O formation in both soils, which we try to elucidate in the theoretical model presented below.

3.5 The mechanism of oxygen isotope fractionation – a fractionation model

To better understand the mechanism of oxygen isotope fractionation and the relation between the apparent isotope effect and the extent of isotope exchange we applied a simulation calculation where the total isotope effect was calculated from the theoretical isotope fractionation associated with two enzymatic reduction steps: NIR and NOR. This model was based on the calculations presented by Rohe et al. (2014a) for pure fungal cultures, where this approach has been described in detail. The model assumes that $\delta^{18}O(N_2O)$ is determined by two isotope fractionation processes associated (i) with the branching isotope effect (ε_n) and

(ii) with the isotope effect due to isotope exchange with soil water (ε_w), both possible at NIR or NOR. This can be expressed by the following isotope mass balance equations:

$$1+\delta = x_{NOR}(1+\delta_w)(1+\varepsilon_w) + (1-x_{NOR})(1+\delta_{NO})(1+\varepsilon_{NOR}) \quad (7)$$

$$1+\delta_{NO} = x_{NIR}(1+\delta_w)(1+\varepsilon_w) + (1-x_{NIR})(1+\delta_n)(1+\varepsilon_{NIR}) \quad (8)$$

where:

$$1-x = (1-x_{NIR})(1-x_{NOR}) \quad (9)$$

$$1+\varepsilon_n = (1+\varepsilon_{NIR})(1+\varepsilon_{NOR}) \quad (10)$$

After substitution and transformation, this gives

$$\frac{\delta-\delta_w}{1+\delta_w} = (1-x)(1+\varepsilon_n)\frac{\delta_n-\delta_w}{1+\delta_w} + (x-x_{NOR})\varepsilon_{NOR}(1+\varepsilon_w) + x\varepsilon_w + (1-x)\varepsilon_n \quad (11)$$

We neglected the possible fractionation associated with the NAR reduction, *i.e.* $\delta(NO_2^-) = \delta(NO_3^-) = \delta_n$ in Eq. (11). This enzymatic step was investigated by Rohe et al. (2014a), and appeared to have no significant impact on the total oxygen fractionation, *i.e.* the branching fractionation for nitrate treatments was in no case higher than for nitrite treatment. This indicates that the oxygen fractionation between nitrate and nitrite is low due to cancellation of the intramolecular effect of about 30 ‰ (Casciotti et al. 2007) by the intermolecular effect when the nitrate pool is not completely consumed. Hence, we only focused here on differentiating between NIR and NOR enzymatic reduction steps, which are most likely the enzymatic reactions crucial for determining final N_2O isotopic values (Kool et al., 2007).

There are many unknown factors in the Eq. (11); first of all, isotopic fractionation factors ε_n and ε_w. We have compiled the results of both methods applied for Exp 1 data: $\delta^{18}O$ method and $\Delta^{17}O$ method to estimate these factors. Using $\delta^{18}O$ method ε was determined from the intercept in Fig. 2 and this value represents total fractionation: $\varepsilon = x\,\varepsilon_w + (1-x)\,\varepsilon_n$ (see Sect. 2.4.1). Using the $\Delta^{17}O$ method, individual x values were calculated for each sample. We have also measured $\delta^{18}O(N_2O/H_2O)$ and $\delta^{18}O(NO_3^-/H_2O)$ for each sample, hence from the transformed Eq. (3):

$$\frac{\delta-\delta_w}{1+\delta_w} = (1-x)(1+\varepsilon_n)\frac{\delta_n-\delta_w}{1+\delta_w} + x\varepsilon_w + (1-x)\varepsilon_n \quad (12)$$

and knowing that $x\ \varepsilon_w + (1- x)\ \varepsilon_n = 0.0182$ for Exp 1.1 and $x\ \varepsilon_w + (1- x)\ \varepsilon_n = 0.0171$ for Exp 1.2 (Fig. 2) we have calculated ε_w and ε_n for each sample. Table 3 summarises the results:

[Table 3]

The determination of ε_w is very precise, with no significant difference between Exp 1.1 and 1.2 ($p = 0.868$). The value obtained (17.5±0.7) ‰ is within the range of the previous values determined for chemical exchange $\varepsilon(NO_2^-/H_2O)$ = 14 ‰ and $\varepsilon(NO_3^-/H_2O)$ = 23 ‰ (Böhlke et al., 2003; Casciotti et al., 2007). So far there are no data for the isotope effect of chemical exchange $\varepsilon(NO/H_2O)$. Therefore, we assumed equal ε_w values for isotope exchange associated with NIR and NOR, similarly to previous studies (Rohe et al., 2014a; Snider et al., 2012). Hence, the ε_w value determined here is a hypothetical mean value of enzymatically mediated isotope exchange associated with NIR ($\varepsilon_w(NO_2^-/H_2O)$) and NOR ($\varepsilon_w(NO/H_2O)$).

ε_n is also quite stable with a weak ($p = 0.006$) and very small (below 1 ‰) difference between Exp 1.1 and 1.2. The ε_n values found are very low and vary around 0, from -1.9 to 2.1 ‰. This is much lower than in previous studies, which reported ε_n from 10 to 30 ‰ (Casciotti et al., 2007; Rohe et al., 2014a).

We checked how well these calculated values fit for the individual samples of both experiments. We started with the simplest Scenario 0, where we assume the values determined in Table 3 for ε_w and ε_n and calculate the $\delta^{18}O(N_2O)$ with Eq. (11), which is then compared with the measured $\delta^{18}O(N_2O)$ and the difference between measured and calculated $\delta^{18}O(N_2O)$ value (D) is determined (Table 4). Since the mean value of 0 was assumed for ε_n in this scenario, the isotope exchange can be associated either with NIR or NOR without any effect on the final $\delta^{18}O(N_2O)$, because Eq. (11) is simplified to:

$$\frac{\delta - \delta_w}{1+\delta_w} = (1-x)\frac{\delta_n - \delta_w}{1+\delta_w} + x\varepsilon_w \qquad (13)$$

This scenario works quite well for Exp 1 data with the maximal D of 1.4 ‰. However, for Exp 2 data we obtain significant overestimation of the calculated $\delta^{18}O(N_2O)$ values for sandy soils (Exp 2.1 and 2.2) up to 6.1 ‰ and underestimation for two other soils, reaching up to 12.2 ‰ for organic soil (Exp 2.5). Why the model developed based on Exp 1 data do not

work for Exp 2 data? We expect that the ε_w value should be quite stable for all the samples. It was observed in the study by Casciotti et al. (2007) that $\varepsilon(NO_2^-/H_2O)$ values varied in a very narrow range. Also in our study in Fig. 2 we obtained very good correlation with stable slope which suggests that the ε_w value must be very stable and almost identical for all the samples. It can be supposed that rather ε_n values can be more variable, but due to nearly complete isotope exchange in Exp 1 these potential variations cannot be reflected in $\delta^{18}O(N_2O)$ values. Also, the study by Rohe et al. (2014a) indicated possibly wide variations of ε_n from 10 to 30 ‰.

[Table 4]

Therefore, for the next scenarios (Scenario 1, 2 and 3 - Table 4) we assumed stable ε_w value of 17.5 ‰, as determined from Exp 1 (Table 3) and ε_n values were calculated individually for each sample with Eq. (11) from the $\delta_0^{18}O(N_2O/H_2O)$ values. In each scenario ε_n was equally distributed between NIR and NOR according to Eq. (10), so that $\varepsilon_{NIR} = \varepsilon_{NOR}$. For our samples we know the value of total isotope exchange (x determined with $\Delta^{17}O$ method), but we do not know at which enzymatic step(s) this exchange occurred. Since the isotope exchange has very different impact on the final $\delta^{18}O(N_2O)$ when associated with NIR or NOR, we can obtain this information by comparing different scenarios (Table 4). In Scenario 1 the total isotope exchange is associated with the first reduction step NIR and in Scenario 2, with the final reduction step NOR. In Scenario 3 the total isotope exchange is equally distributed between both steps NIR and NOR according to Eq. (9) so that $x_{NIR} = x_{NOR}$.

In this study, we could not determine at which enzymatic step isotope exchange occurs, but only its impact on the implied isotope effects. Namely, in Scenario 1 the exchange effect associated with x_{NIR} precedes the branching effect at NOR (ε_{NOR}) and, conversely, in Scenario 2 the exchange isotope effect associated with x_{NOR} occurs after both branching effects (ε_{NIR}, ε_{NOR}). Hence, in Scenario 1 ε_{NOR} has a more direct impact on the final $\delta^{18}O(N_2O)$ whereas in Scenario 2 the last fractionation step is related to ε_w (Eq. (11)). Therefore, applying different scenarios results in different values for the calculated ε_n (Table 4).

The narrowest range of variations of the calculated ε_n values was obtained in Scenario 1. For Exp 1 they vary around 0, similarly to the results presented in Table 3, which indicates that

this model and the equations applied for $\delta^{18}O$ method (Eq. (12)) are actually the same. For Exp 2 the calculated ε_n values are negative for sandy soils (Exp 2.1 and 2.2) from -9.1 to -6.2 ‰ and positive for other soils with lower values for silt loam from 1.6 to 3.8 ‰ and higher for organic soil from 3.8 to 18.1 ‰ (Table 4). Variations of calculated ε_n values are much larger in Scenario 2 with a particularly wide range for Exp 1 from -72.8 to +38.5 ‰. For Exp. 2, a similar trend as in Scenario 1 is observed, with negative values for sandy soils (down to -20.0 ‰) and highest values for organic soil (up to 37.1 ‰). The absolute values are generally larger and the variations among them are thereby increased when compared to Scenario 1. The strongly negative ε_n values obtained for Scenario 2 are outside the range of plausible range based on previous determinations (Casciotti et al., 2007; Rohe et al., 2014a). Moreover, for the last sample of Exp 1 where x=1 this scenario fails in finding the ε_n value for D=0, because for complete isotope exchange by NOR, the associated branching isotope effect has no impact on the final $\delta^{18}O(N_2O)$. But still Scenario 1 is more plausible because (i) the overall ε_n variations are smaller and (ii) we do not find extremely negative values. Results from Scenario 3 are situated in the middle of Scenario 1 and 2, and show larger variations than Scenario 1, but without the extreme outliers, hence can be also a plausible model. From comparison of these scenarios we can say that isotope exchange is likely associated with NIR and may also partially take place at NOR (but not NOR alone). This reinforces the previous findings from pure culture studies which suggested the majority of isotope exchange associated mainly with nitrite reduction (Garber and Hollocher, 1982; Rohe et al., 2014a). Moreover, each scenario indicates clearly a much lower branching effect for the two sandy soils in Exp. 2 when compared to silt loam and organic soil. This is the reason behind the different slope of correlation $\delta_0^{18}O(N_2O/H_2O)$ *vs.* x in Fig. 4 for sandy soils. Lower ε_n values mean that N_2O is less enriched in ^{18}O in relation to soil nitrate and lower x results in smaller increase in $\delta^{18}O(N_2O)$ values, which was observed for sandy soils (Fig.4).

For each scenario our model indicated rather lower ε_n values than previously assumed (Casciotti et al., 2007; Rohe et al., 2014a). But actually, the isotope effect determined by Casciotti et al. (2007), +25 to +30 ‰, takes only the intra-molecular branching effect into account, because in the bacterial denitrification method the whole nitrate pool is quantitatively consumed, hence the inter-molecular isotope effect cannot manifest. Therefore, the values found by Casciotti et al. (2007) represent the maximal possible branching effect. In the experiment presented by Rohe et al. (2014a) only very little added substrate was reduced,

hence we should also observe the inter-molecular isotope effects. Indeed, the model applied by Rohe et al. (2014a) indicated lower magnitudes for net branching, down to +10 ‰ for ε_{NIR} and 0 ‰ for ε_{NAR}. This may suggest that the net branching effect decreases with smaller reaction rates because of inter-molecular isotope effects. But are negative net branching effects actually possible? The answer is yes, provided that the inter-molecular effect exceeds the intra-molecular effect, *i.e.* the former must be more negative than -30 ‰. An idea about the magnitude of the intermolecular effect can be obtained from the change in isotopic signature of the remaining nitrate, since this reflects the enrichment in residual nitrate-^{18}O due to intermolecular effects. In pure culture studies this effect ranges from -23 to -5 ‰ (Granger et al., 2008), but in soil incubations values as low as -37 ‰ has been observed (Exp. 1F in Lewicka-Szczebak et al. (2014)). Hence, slightly negative net ε_n values are theoretically possible, but up to a few ‰ for each enzymatic step, which gives the minimal overall ε_n of about -10 ‰. Therefore, the results of Scenario 2 must be rejected, whereas the values found in Scenario 1 are most plausible.

3.6 Significance for quantification and differentiation of soil denitrification

From the presented results it is most surprising and incomprehensible, why the same soils show various extents of isotope exchange with soil water, and especially, why this exchange was high and stable under static anoxic conditions and significantly lower in flow-through incubations. Most probably, in the static inhibited experiments denitrification is the only N_2O producing process and in the flow-through uninhibited incubations other N_2O producing processes may significantly contribute to N_2O production. These incubations were performed initially under oxic conditions, which were switched to anoxic conditions after three days. However, all the results presented here originate from this anoxic phase, since the N_2O production during oxic phase was too low for $\Delta^{17}O$ analyses. Hence, the potentially contributing processes might be fungal denitrification, co-denitrification, nitrifier denitrification or dissimilatory nitrate reduction to ammonium (DNRA). ^{15}N site preference ($\delta^{15}N^{sp}$) may be used as a tracer to distinguish some of these processes. It is known that fungal denitrification and nitrification are characterized by significantly higher $\delta^{15}N^{sp}$ values (33 to 37 ‰ (Rohe et al., 2014a; Sutka et al., 2008; Sutka et al., 2006)) when compared to bacterial denitrification and nitrifier denitrification (-11 to 0 ‰ (Sutka et al., 2006; Toyoda et al., 2005)). To check the hypothesis of mixing of N_2O from various sources we plotted $\delta_0{}^{18}O$ (N_2O/H_2O) values against $\delta_0{}^{15}N^{sp}$ values of produced N_2O (Fig. 5).

[Fig. 5]

It can be clearly noticed that the results from the inhibited experiment (Exp 1, red symbols) fit perfectly into the field of bacterial denitrification. Similarly, the results of sandy soils from the Exp 2 show a slightly wider range, but still are typical for bacterial denitrification. In contrast, silt loam soil (Exp 2.3, 2.4) and organic soil (Exp 2.5, 2.6) both show increased $\delta_0^{18}O(N_2O/H_2O)$ and $\delta_0^{15}N^{sp}$ values which are very well correlated. This could indicate that in Exp 2 another process characterized by high $\delta^{15}N^{sp}$ and $\delta^{18}O$ values has significant contribution to total N_2O production by these two soils. This could be nitrification, which is rather not plausible due to the anoxic conditions, or fungal denitrification. But it remains unclear why this was not observed in the inhibited static incubation for the same soil (silt loam). C_2H_2 inhibition do not affect fungal denitrification (Maeda et al., 2015) as far as NO_3^- and NO_2^- availability is not restricted by inhibited nitrification. However, in the flow-through incubations, the first oxic phase might have activated other microorganisms, possibly preferentially fungi. This could explain that their contribution is observed only in Exp 2 but not in Exp 1. Such an activation of denitrification by oxygen supply has been documented for one fungus species (Zhou et al., 2001).

We verified if the correlation presented in Fig. 5 could have resulted from calculation artifacts, since all of the higher $\delta_0^{18}O(N_2O/H_2O)$ and $\delta_0^{15}N^{sp}$ values were corrected for N_2O reduction (according to the method described in Sect. 2.5). This correction method does not provide very precise results, since the isotope effects associated with N_2O reduction are not entirely stable and predictable (Lewicka-Szczebak et al., 2015; Lewicka-Szczebak et al., 2014). Therefore, we have checked if this correlation may be only a calculation artifact and recalculated the values assuming larger range of isotopic fractionations (±5 ‰, resulting in $\varepsilon^{15}N^{sp}(N_2/N_2O)$ from -10 to 0 ‰ and $\varepsilon^{18}O(N_2/N_2O)$ from -20 to -6 ‰). Results show that the correlation may slightly change in slope (from 0.41 to 0.85), intercept (from -10.4 to -18.0) and significance (R^2 from 0.64 to 0.91). But it always keeps the same trend, *i.e.* for the Exps 2.3 - 2.6 we obtain in any case correlated increase of $\delta_0^{15}N^{sp}$ and $\delta_0^{18}O(N_2O/H_2O)$ (see grey dashed lines in Fig. 5), proving that the indication for further contributing processes cannot be an artifact of the correction approach. For these experiments (2.3-2.6) in our model calculations (Table 4) always higher ε_n values were found when compared to Exp 1 and 2.1-

2.2. Also for pure culture studies of fungal denitrification the ε_n values determined by a similar modeling approach were higher, up to 30 ‰ (Rohe et al., 2014a). This would support the hypothesis on fungal denitrification contribution.

3.7 Source of $\Delta^{17}O$ in atmospheric N_2O

In Exp 1 the $\Delta^{17}O(N_2O)$ values obtained from all measured N_2O samples were very low. Moreover, we also included the treatment with chemical nitrate as fertilizer, characterised by slightly negative $\Delta^{17}O$ excess (of ca.-1.5‰), and the produced N_2O did not show any positive $\Delta^{17}O$ excess (results not shown). The produced N_2O is always characterised by smaller ^{17}O-excess ($\Delta^{17}O$ values closer to 0) than in the source nitrate (Table 1). These results indicate that denitrification produces N_2O of randomly distributed oxygen, due to mostly very high extent of isotope exchange with soil water and the consequent loss of ^{17}O excess of nitrate. However, in Exp 2 numerous samples showed lower extent of isotope exchange, down to 50 %, and the ^{17}O excess of nitrate is partially transferred to N_2O, resulting in $\Delta^{17}O(N_2O)$ up to 5 ‰. This indicates that denitrification may be potentially the source of atmospheric N_2O with ^{17}O excess, as previously supposed (Kaiser et al., 2004; Michalski et al., 2003), but the magnitude of this excess is largely reduced by the exchange of oxygen isotopes with randomly distributed soil water.

4. Conclusions

It can be supposed that bacterial denitrification in soils is characterised by quite stable $\delta_0^{18}O(N_2O/H_2O)$ of 17.5 ± 1.2 ‰ due to the nearly complete O isotope exchange and constant isotope effect associated with this exchange. Hence, when N_2O producing processes other than heterotrophic processes are negligible, $\delta_0^{18}O(N_2O)$ can be well predicted. Conversely, $\delta_0^{18}O(N_2O/H_2O)$ values larger than 19 ‰ are probably indicative for the contribution of other processes. However, more work on oxygen isotope effects during N_2O production by various microorganisms is needed to obtain robust estimate of their contribution. It is necessary to conduct experiments to determine the possible range of $\delta_0^{18}O(N_2O/H_2O)$ for different N_2O forming processes. From the studies available until now, we can make a first estimate for $\delta_0^{18}O(N_2O/H_2O)$ characteristic of fungal denitrification of (48.2±3.7) ‰ (when disregarding two most extreme values; for all results (47.4±10.3) ‰) (Rohe et al., 2014a). This value is very different from the $\delta_0^{18}O(N_2O/H_2O)$ of bacterial denitrification determined here, i.e.

(17.5±1.2) ‰. This opens up a new perspective of applying $\delta_0^{18}O(N_2O/H_2O)$ for differentiation between fungal and bacterial denitrification.

Acknowledgements

This study was supported by German Research Foundation (DFG We/1904-4). Many thanks are due to Anette Giesemann and Martina Heuer for help in N_2O isotopic analyses; Lars Szwec for $\Delta^{17}O$ analyses; Kerstin Gilke for help in chromatographic analyses, Caroline Buchen for supplying soil for laboratory incubations and Maciej Lewicki for supplying the isotopically depleted water from the Tatra Mountains, Poland.

References

Böhlke, J. K., Mroczkowski, S. J., and Coplen, T. B.: Oxygen isotopes in nitrate: new reference materials for ^{18}O: ^{17}O: ^{16}O measurements and observations on nitrate-water equilibration, Rapid Commun Mass Sp, 17, 1835-1846, 2003.

Butterbach-Bahl, K., Willibald, G., and Papen, H.: Soil core method for direct simultaneous determination of N_2 and N_2O emissions from forest soils, Plant Soil, 240, 105-116, 2002.

Casciotti, K. L., Bohlke, J. K., McIlvin, M. R., Mroczkowski, S. J., and Hannon, J. E.: Oxygen isotopes in nitrite: Analysis, calibration, and equilibration, Anal Chem, 79, 2427-2436, 2007.

Casciotti, K. L., Sigman, D. M., Hastings, M. G., Bohlke, J. K., and Hilkert, A.: Measurement of the oxygen isotopic composition of nitrate in seawater and freshwater using the denitrifier method, Anal Chem, 74, 4905-4912, 2002.

Dyckmans, J., Lewicka-Szczebak, D., Szwec, L., Langel, R., and Well, R.: Comparison of methods to determine triple oxygen isotope composition of N2O, Rapid Commun Mass Sp, 29, 1991-1996, 2015.

Eickenscheidt, T., Heinichen, J., Augustin, J., Freibauer, A., and Drosler, M.: Nitrogen mineralization and gaseous nitrogen losses from waterlogged and drained organic soils in a black alder (Alnus glutinosa (L.) Gaertn.) forest, Biogeosciences, 11, 2961-2976, 2014.

Garber, E. A. E. and Hollocher, T. C.: ^{15}N, ^{18}O Tracer Studies on the Activation of Nitrite by Denitrifying Bacteria - Nitrite Water-Oxygen Exchange and Nitrosation Reactions as Indicators of Electrophilic Catalysis, J Biol Chem, 257, 8091-8097, 1982.

Granger, J., Sigman, D. M., Lehmann, M. F., and Tortell, P. D.: Nitrogen and oxygen isotope fractionation during dissimilatory nitrate reduction by denitrifying bacteria, Limnol Oceanogr, 53, 2533-2545, 2008.

IPCC: The Physical Science Basis. Contribution of Working Group I to the Fifth Assessment Report of the Intergovernmental Panel on Climate Change., Intergovernmental Panel on Climate Change, Cambridge, United Kingdom and New York, NY, USA, 996 pp., 1553 pp., 2013.

Kaiser, J., Hastings, M. G., Houlton, B. Z., Rockmann, T., and Sigman, D. M.: Triple oxygen isotope analysis of nitrate using the denitrifier method and thermal decomposition of N_2O, Anal Chem, 79, 599-607, 2007.

Kaiser, J. and Röckmann, T.: Correction of mass-spectrometric isotope ratio measurements for isobaric isotopologues of O_2, CO, CO_2, N_2O and SO_2, Rapid Commun. Mass Spectrom., 22, 3997-4008, 2008.

Kaiser, J., Rockmann, T., and Brenninkmeijer, C. A. M.: Contribution of mass-dependent fractionation to the oxygen isotope anomaly of atmospheric nitrous oxide, J Geophys Res-Atmos, 109, 2004.

Königer, P., Marshall, J. D., Link, T., and Mulch, A.: An inexpensive, fast, and reliable method for vacuum extraction of soil and plant water for stable isotope analyses by mass spectrometry, Rapid Commun Mass Sp, 25, 3041-3048, 2011.

Kool, D. M., Wrage, N., Oenema, O., Dolfing, J., and Van Groenigen, J. W.: Oxygen exchange between (de) nitrification intermediates and H_2O and its implications for source determination of NO_3^- and N_2O: a review, Rapid Commun Mass Sp, 21, 3569-3578, 2007.

Kool, D. M., Wrage, N., Oenema, O., Harris, D., and Van Groenigen, J. W.: The ^{18}O signature of biogenic nitrous oxide is determined by O exchange with water, Rapid Commun Mass Sp, 23, 104-108, 2009.

Lewicka-Szczebak, D., Well, R., Bol, R., Gregory, A., Matthews, P., Misselbrook, T., Whalley, R., and Cardenas, L.: Isotope fractionation factors controlling isotopocule signatures

of soil-emitted N_2O produced by denitrification processes of various rates, Rapid Commun Mass Sp, 29, 269–282, 2015.
Lewicka-Szczebak, D., Well, R., Giesemann, A., Rohe, L., and Wolf, U.: An enhanced technique for automated determination of ^{15}N signatures of N_2, (N_2+N_2O) and N_2O in gas samples, Rapid Commun Mass Sp, 27, 1548-1558, 2013.
Lewicka-Szczebak, D., Well, R., Koster, J. R., Fuss, R., Senbayram, M., Dittert, K., and Flessa, H.: Experimental determinations of isotopic fractionation factors associated with N_2O production and reduction during denitrification in soils, Geochim Cosmochim Ac, 134, 55-73, 2014.
Maeda, K., Spor, A., Edel-Hermann, V., Heraud, C., Breuil, M. C., Bizouard, F., Toyoda, S., Yoshida, N., Steinberg, C., and Philippot, L.: N_2O production, a widespread trait in fungi, Sci Rep-Uk, 5, 2015.
Mariotti, A., Germon, J. C., Hubert, P., Kaiser, P., Letolle, R., Tardieux, A., and Tardieux, P.: Experimental determination of nitrogen kinetic isotope fractionation - some principles - illustration for the denitrification and nitrification processes, Plant Soil, 62, 413-430, 1981.
Michalski, G., Scott, Z., Kabiling, M., and Thiemens, M. H.: First measurements and modeling of Delta ^{17}O in atmospheric nitrate, Geophys Res Lett, 30, 2003.
Mohn, J., Wolf, B., Toyoda, S., Lin, C. T., Liang, M. C., Bruggemann, N., Wissel, H., Steiker, A. E., Dyckmans, J., Szwec, L., Ostrom, N. E., Casciotti, K. L., Forbes, M., Giesemann, A., Well, R., Doucett, R. R., Yarnes, C. T., Ridley, A. R., Kaiser, J., and Yoshida, N.: Interlaboratory assessment of nitrous oxide isotopomer analysis by isotope ratio mass spectrometry and laser spectroscopy: current status and perspectives, Rapid Commun Mass Sp, 28, 1995-2007, 2014.
Opdyke, M. R., Ostrom, N. E., and Ostrom, P. H.: Evidence for the predominance of denitrification as a source of N_2O in temperate agricultural soils based on isotopologue measurements, Global Biogeochem Cy, 23, GB4018, 2009.
Ostrom, N. E., Pitt, A., Sutka, R., Ostrom, P. H., Grandy, A. S., Huizinga, K. M., and Robertson, G. P.: Isotopologue effects during N_2O reduction in soils and in pure cultures of denitrifiers, J Geophys Res-Biogeo, 112, G02005, 2007.
Park, S., Perez, T., Boering, K. A., Trumbore, S. E., Gil, J., Marquina, S., and Tyler, S. C.: Can N_2O stable isotopes and isotopomers be useful tools to characterize sources and microbial pathways of N_2O production and consumption in tropical soils?, Global Biogeochem Cy, 25, GB1001, 2011.
Perez, T., Garcia-Montiel, D., Trumbore, S., Tyler, S., De Camargo, P., Moreira, M., Piccolo, M., and Cerri, C.: Nitrous oxide nitrification and denitrification ^{15}N enrichment factors from Amazon forest soils, Ecol Appl, 16, 2153-2167, 2006.
Ravishankara, A. R., Daniel, J. S., and Portmann, R. W.: Nitrous Oxide (N_2O): The Dominant Ozone-Depleting Substance Emitted in the 21st Century, Science, 326, 123-125, 2009.
Röckmann, T., Kaiser, J., Brenninkmeijer, C. A. M., and Brand, W. A.: Gas chromatography/isotope-ratio mass spectrometry method for high-precision position-dependent ^{15}N and ^{18}O measurements of atmospheric nitrous oxide, Rapid Commun Mass Sp, 17, 1897-1908, 2003.
Rohe, L., Anderson, T.-H., Braker, G., Flessa, H., Giesemann, A., Lewicka-Szczebak, D., Wrage-Mönnig, N., and Well, R.: Dual isotope and isotopomer signatures of nitrous oxide from fungal denitrification – a pure culture study, Rapid Commun Mass Sp, 28, 1893-1903, 2014a.
Rohe, L., Anderson, T. H., Braker, G., Flessa, H., Giesemann, A., Wrage-Monnig, N., and Well, R.: Fungal oxygen exchange between denitrification intermediates and water, Rapid Commun Mass Sp, 28, 377-384, 2014b.

Schmidt, H. L., Werner, R. A., Yoshida, N., and Well, R.: Is the isotopic composition of nitrous oxide an indicator for its origin from nitrification or denitrification? A theoretical approach from referred data and microbiological and enzyme kinetic aspects, Rapid Commun Mass Sp, 18, 2036-2040, 2004.
Scholefield, D., Hawkins, J. M. B., and Jackson, S. M.: Development of a helium atmosphere soil incubation technique for direct measurement of nitrous oxide and dinitrogen fluxes during denitrification, Soil Biol Biochem, 29, 1345-1352, 1997.
Snider, D., Venkiteswaran, J. J., Schiff, S. L., and Spoelstra, J.: A new mechanistic model of $\delta^{18}O$-N_2O formation by denitrification, Geochim Cosmochim Ac, 112, 102-115, 2013.
Snider, D. M., Schiff, S. L., and Spoelstra, J.: $^{15}N/^{14}N$ and $^{18}O/^{16}O$ stable isotope ratios of nitrous oxide produced during denitrification in temperate forest soils, Geochim Cosmochim Ac, 73, 877-888, 2009.
Snider, D. M., Venkiteswaran, J. J., Schiff, S. L., and Spoelstra, J.: Deciphering the oxygen isotope composition of nitrous oxide produced by nitrification, Global Change Biol, 18, 356-370, 2012.
Stein, L. Y. and Yung, Y. L.: Production, isotopic composition, and atmospheric fate of biologically produced nitrous oxide, Annu Rev Earth Pl Sc, 31, 329-356, 2003.
Sutka, R. L., Adams, G. C., Ostrom, N. E., and Ostrom, P. H.: Isotopologue fractionation during N_2O production by fungal denitrification, Rapid Commun Mass Sp, 22, 3989-3996, 2008.
Sutka, R. L., Ostrom, N. E., Ostrom, P. H., Breznak, J. A., Gandhi, H., Pitt, A. J., and Li, F.: Distinguishing nitrous oxide production from nitrification and denitrification on the basis of isotopomer abundances, Appl Environ Microb, 72, 638-644, 2006.
Sutka, R. L., Ostrom, N. E., Ostrom, P. H., Gandhi, H., and Breznak, J. A.: Nitrogen isotopomer site preference of N_2O produced by Nitrosomonas europaea and Methylococcus capsulatus Bath, Rapid Commun Mass Sp, 17, 738-745, 2003.
Toyoda, S., Mutobe, H., Yamagishi, H., Yoshida, N., and Tanji, Y.: Fractionation of N_2O isotopomers during production by denitrifier, Soil Biol Biochem, 37, 1535-1545, 2005.
Toyoda, S., Yano, M., Nishimura, S., Akiyama, H., Hayakawa, A., Koba, K., Sudo, S., Yagi, K., Makabe, A., Tobari, Y., Ogawa, N. O., Ohkouchi, N., Yamada, K., and Yoshida, N.: Characterization and production and consumption processes of N_2O emitted from temperate agricultural soils determined via isotopomer ratio analysis, Global Biogeochem Cy, 25, GB2008, 2011.
Toyoda, S. and Yoshida, N.: Determination of nitrogen isotopomers of nitrous oxide on a modified isotope ratio mass spectrometer, Anal Chem, 71, 4711-4718, 1999.
Well, R. and Flessa, H.: Isotopologue enrichment factors of N_2O reduction in soils, Rapid Commun Mass Sp, 23, 2996-3002, 2009.
Well, R., Flessa, H., Xing, L., Ju, X. T., and Romheld, V.: Isotopologue ratios of N_2O emitted from microcosms with NH_4^+ fertilized arable soils under conditions favoring nitrification, Soil Biol Biochem, 40, 2416-2426, 2008.
Westley, M. B., Popp, B. N., and Rust, T. M.: The calibration of the intramolecular nitrogen isotope distribution in nitrous oxide measured by isotope ratio mass spectrometry, Rapid Commun Mass Sp, 21, 391-405, 2007.
Zhou, Z. M., Takaya, N., Sakairi, M. A. C., and Shoun, H.: Oxygen requirement for denitrification by the fungus Fusarium oxysporum, Arch Microbiol, 175, 19-25, 2001.

Table 1. Exp 1 results: soil moisture (expressed as water filled pore space: WFPS), N_2O+N_2 production rate (expressed as mass of N as sum of N_2O and N_2 per mass of dry soil per time), ^{17}O excess in soil nitrate ($\Delta^{17}O(NO_3)$) and in N_2O ($\Delta^{17}O(N_2O)$) with calculated exchange with soil water (x), and oxygen isotopic signature ($\delta^{18}O$) of soil nitrate (NO_3^-), soil water (H_2O) and N_2O with calculated isotope ratio difference between soil water and N_2O ($\delta_0{}^{18}O$ (N_2O/H_2O)). For samples with non-inhibited N_2O reduction the N_2O mole fraction ($f(N_2O)$) was taken into account to calculate the $\delta^{18}O$ unaffected by N_2O reduction ($\delta_0{}^{18}O(N_2O)$) and the respective $\delta_0{}^{18}O(N_2O/H_2O)$. Only Chile Saltpeter treatments are presented, for which the individual determination of x was possible. Part of the data from Exp 1.1 ($\delta^{18}O(NO_3^-)$, $\delta^{18}O(H_2O)$, $\delta^{18}O(N_2O)$) was already published in (Lewicka-Szczebak et al., 2014).

treatment		N_2O+N_2 production rate	$\Delta^{17}O(NO_3^-)$	$\Delta^{17}O(N_2O)$	x [%]	$\delta^{18}O(NO_3)$	$\delta^{18}O(H_2O)$	$\delta^{18}O(N_2O)$	$f(N_2O)^a$	$\delta_0{}^{18}O$ $(N_2O)^b$	$\delta_0{}^{18}O$ (N_2O/H_2O)
WFPS [%]	inhibition	[μg kg^{-1} h^{-1}]	[‰]	[‰]		[‰]	[‰]	[‰]		[‰]	[‰]
Exp 1.1 a, loamy sand, 8 ºC											
80		114	11.9 ± 0.6	0.4 ± 0.5	96.2 ± 4.7	38.8±0.5	-9.2±0.5	13.4 ± 0.2	0.84±0.04	10.4	19.7 ± 0.5
80	C_2H_2	107	11.9 ± 0.6	0.8 ± 0.4	93.1 ± 3.1	38.8±0.5	-9.2±0.5	10.4 ± 0.1	1	10.4	19.8 ± 0.5
80		125	11.9 ± 0.6	0.8 ± 0.2	92.7 ± 1.1	37.5±0.5	-13.5±0.5	8.4 ± 0.3	0.84±0.04	5.4	19.1 ± 0.6
80	C_2H_2	126	11.9 ± 0.6	0.3 ± 0.7	96.2 ± 3.4	37.5±0.5	-13.5±0.5	5.7 ± 0.0	1	5.7	19.4 ± 0.5
Exp 1.1b, loamy sand, 22 ºC											
80		427	10.4 ± 0.8	0.4 ± 0.2	95.7 ± 1.8	42.6±0.5	-9.2±0.5	12.5 ± 0.2	0.85±0.06	9.6	19.0 ± 0.5
80	C_2H_2	362	10.4 ± 0.8	0.4 ± 0.0	96.4 ± 0.2	42.6±0.5	-9.2±0.5	9.5 ± 0.0	1	9.5	18.9 ± 0.5
80		429	10.4 ± 0.8	0.2 ± 0.1	98.2 ± 1.5	42.1±0.5	-13.5±0.5	7.5 ± 0.1	0.85±0.06	4.7	18.4 ± 0.5
80	C_2H_2	370	10.4 ± 0.8	0.5 ± 0.1	94.8 ± 0.5	42.1±0.5	-13.5±0.5	4.5 ± 0.1	1	4.5	18.3 ± 0.5
Exp 1.1 c, silt loam, 22 ºC											
80		266	9.2 ± 1.3	0.0 ± 0.2	99.5 ± 0.9	31.8±0.5	-2.6±0.5	26.4 ± 0.1	0.57±0.03	16.4	19.1 ± 0.5
80	C_2H_2	257	9.2 ± 1.3	0.4 ± 0.1	95.3 ± 1.4	31.8±0.5	-2.6±0.5	15.9 ± 0.1	1	15.9	18.5 ± 0.5
80		271	9.2 ± 1.3	0.1 ± 0.2	98.6 ± 1.3	31.8±0.5	-8.7±0.5	20.7 ± 0.2	0.57±0.03	10.8	19.7 ± 0.5
80	C_2H_2	251	9.2 ± 1.3	0.4 ± 0.1	95.0 ± 1.5	31.8±0.5	-8.7±0.5	9.8 ± 0.1	1	9.8	18.7 ± 0.5
Exp 1.2 a, loamy sand, 22 ºC											
80	C_2H_2	126	3.4 ± 0.5	n.d.	n.d.	6.5±0.5	-10.4±0.5	6.3 ± 0.1	1	6.3	16.9 ± 0.5

65	C_2H_2	112	3.4 ± 0.5	0.2 ± 0.3	92.6 ± 8.5	6.5±0.5	-10.1±0.5	6.9 ± 0.2	1	6.9	17.2 ± 0.5
50	C_2H_2	50	3.4 ± 0.5	0.0 ± 0.3	95.8 ± 3.9	6.5±0.5	-8.9±0.5	7.6 ± 0.3	1	7.6	16.6 ± 0.6
80	C_2H_2	161	3.4 ± 0.5	n.d.	n.d.	6.5±0.5	-5.0±0.5	10.5 ± 0.0	1	10.5	15.6 ± 0.5
65	C_2H_2	102	3.4 ± 0.5	0.2 ± 0.2	92.7 ± 5.2	6.5±0.5	-5.7±0.5	11.6 ± 0.1	1	11.6	17.5 ± 0.5
50	C_2H_2	74	3.4 ± 0.5	0.2 ± 0.2	94.5 ± 5.1	6.5±0.5	-6.6±0.5	10.7 ± 0.1	1	10.7	17.4 ± 0.5
Exp 1.2 b, silt loam, 22 ºC											
80	C_2H_2	137	2.6 ± 0.4	0.2 ± 0.2	90.6 ± 7.3	3.2±0.5	-8.1±0.5	8.3 ± 0.1	1	8.3	16.5 ± 0.5
65	C_2H_2	130	2.6 ± 0.4	0.2 ± 0.1	92.2 ± 3.7	3.2±0.5	-7.1±0.5	9.8 ± 0.1	1	9.8	17.1 ± 0.5
50	C_2H_2	121	2.6 ± 0.4	0.1 ± 0.1	96.5 ± 4.3	3.2±0.5	-5.9±0.5	12.5 ± 0.2	1	12.5	18.6 ± 0.5
80	C_2H_2	111	2.6 ± 0.4	-0.1 ± 0.1	99.1 ± 1.6	3.2±0.5	-1.6±0.5	15.1 ± 0.2	1	15.1	16.7 ± 0.6
65	C_2H_2	132	2.6 ± 0.4	0.0 ± 0.1	98.4 ± 1.6	3.2±0.5	-1.8±0.5	15.2 ± 0.2	1	15.2	17.0 ± 0.5
50	C_2H_2	106	2.6 ± 0.4	-0.2 ± 0.0	100.0 ± 1.8	3.2±0.5	-2.0±0.5	15.7 ± 0.3	1	15.7	17.7 ± 0.6

[a] $c(N_2O)/[c(N_2)+c(N_2O)]$: based on parallel ^{15}N treatment (last sampling results)

[b] N_2O reduction not inhibited, the values are corrected taking into account product ratio and isotope fractionation, according to Rayleigh fractionation $^{18}\varepsilon(N_2/N_2O)$ values taken from Lewicka-Szczebak et al. (2014): -17.4 ‰ (see Sect. 2.5 for details)

Table 2. Exp 2 results: soil moisture (expressed as water filled pore space: WFPS), N_2O+N_2 production rate (expressed as mass of N as sum of N_2O and N_2 per mass of dry soil per time), ^{17}O excess in soil nitrate ($\Delta^{17}O(NO_3)$) and in N_2O ($\Delta^{17}O(N_2O)$) with calculated exchange with soil water (x) and oxygen isotopic signature ($\delta^{18}O$) of soil nitrate (NO_3), soil water (H_2O) and N_2O. All $\delta^{18}O(N_2O)$ values were corrected taking into account N_2O mole fraction ($f(N_2O)$) to calculate the values unaffected by N_2O reduction ($\delta_0{}^{18}O(N_2O)$) and the respective $\delta_0{}^{18}O(N_2O/H_2O)$.

WFPS [%]	N_2O+N_2 production rate [μg kg^{-1} h^{-1}]	$\Delta^{17}O(NO_3^-)$ [‰]	$\Delta^{17}O(N_2O)$ [‰]	x [%]	$\delta^{18}O(NO_3^-)$ [‰]	$\delta^{18}O(H_2O)$ [‰]	$\delta^{18}O(N_2O)$ [‰]	$f(N_2O)$ [a]	$\delta_0{}^{18}O$ (N_2O) [b] [‰]	$\delta_0{}^{18}O$ (N_2O/H_2O) [‰]
Exp 2.1, sand										
73.6 ± 0.7	91	10.8 ± 0.3	2.7 ± 0.4	73.9 ± 4.2	34.3 ± 1.7	-8.6 ± 0.5	12.1 ± 0.2	0.95 ± 0.01	11.5 ± 0.2	20.2 ± 0.5
			2.6 ± 1.1	74.4 ± 11.0			11.0 ± 0.4	0.92 ± 0.01	10.0 ± 0.5	18.8 ± 0.7
Exp 2.2 loamy sand										
70.4 ± 0.9	49	11.9 ± 0.3	3.7 ± 0.4	66.9 ± 3.1	43.0 ± 2.4	-7.4 ± 0.5	18.4 ± 2.7	0.80 ± 0.05	15.7 ± 2.1	23.3 ± 2.2
			3.3 ± 0.2	71.2 ± 1.6			15.7 ± 0.9	0.83 ± 0.02	13.5 ± 0.7	21.0 ± 0.8
Exp 2.3 silt loam										
78.4 ± 1.9	80	11.3 ± 0.2	5.2 ± 0.2	52.0 ± 2.2	43.1 ± 2.3	-5.3 ± 0.5	43.8 ± 2.2	0.32 ± 0.03	29.4 ± 2.6	34.9 ± 2.6
			5.3 ± 0.1	50.4 ± 1.4			46.1 ± 3.9	0.29 ± 0.10	30.4 ± 0.2	35.9 ± 0.5
Exp 2.4 silt loam										
73.6 ± 1.8	52	12.1 ± 0.3	3.5 ± 0.5	69.9 ± 4.0	52.0 ± 3.3	-5.0 ± 0.5	30.1 ± 0.4	0.68 ± 0.02	25.4 ± 0.7	30.5 ± 0.9
			5.0 ± 0.5	56.3 ± 4.1			37.7 ± 4.1	0.63 ± 0.07	31.9 ± 4.3	37.1 ± 4.3
Exp 2.5 organic										
86.5 ± 1.8	743	7.8 ± 0.2	2.3 ± 1.1	68.1 ± 13.8	30.4 ± 0.6	-6.4 ± 0.5	26.4 ± 5.3	0.60 ± 0.02	20.0 ± 5.1	26.6 ± 5.1
			2.3 ± 0.8	68.2 ± 9.5			37.7 ± 2.9	0.51 ± 0.02	29.3 ± 3.3	36.0 ± 3.3
Exp 2.6 organic										
78.7 ± 0.4	1198	12.5 ± 0.7	1.1 ± 0.2	90.2 ± 1.8	43.6 ± 5.6	-6.7 ± 0.5	18.5 ± 0.0	0.82 ± 0.02	16.1 ± 0.2	22.9 ± 0.6
			2.3 ± 0.3	78.8 ± 3.0			25.6 ± 0.8	0.74 ± 0.05	21.9 ± 1.6	28.7 ± 1.7

[a] $c(N_2O)/[c(N_2)+c(N_2O)]$: based on direct GC measurements in N_2-free atmosphere

[b] initial $\delta^{18}O$ values of unreduced N_2O calculated according to Rayleigh fractionation, $^{18}\varepsilon(N_2/N_2O)$ values taken from Lewicka-Szczebak et al. (2015): -12 ‰ (see Sect. 2.5)

Table 3. Isotopic fractionation factors calculated based on Exp 1 results with Eq. (12) (see text for details). Results presented separately for Exp 1.1 and 1.2 and mean values for both.

	ε_w [‰]	ε_n [‰]
Exp 1.1	17.44 ± 0.71	0.74 ± 0.70
Exp 1.2	17.50 ± 0.67	-0.39 ± 0.66
mean all	17.48 ± 0.66	0.03 ± 0.86

Table 4. Oxygen fractionation model based on the results obtained ($\delta_0^{18}O(N_2O)$) and isotope exchange (x) determined by $\Delta^{17}O$ method and ε_w = 17.5 ‰ determined from Exp 1 data (Table 3). Scenarios with varied ε_n values and x_{NIR} or x_{NOR} (fraction of isotope exchange associated with NIR or NOR) are compared. D is the difference between measured $\delta^{18}O$ of N_2O and the calculated $\delta^{18}O$ of N_2O in a particular scenario.

	Scenario 0: $x = x_{NIR}$ or x_{NOR} **$\varepsilon_n = 0$** ε_w = 17.5 [‰]		**Scenario 1:** $x_{NIR} = x$; $x_{NOR} = 0$ ε_n fitted ε_w = 17.5 [‰]		**Scenario 2:** $x_{NIR} = 0$; $x_{NOR} = x$ ε_n fitted ε_w = 17.5 [‰]		**Scenario 3:** $x_{NIR} = x_{NOR}$ ε_n fitted ε_w = 17.5 [‰]	
	D	**ε_n**	*D*	**ε_n**	*D*	**ε_n**	*D*	
Exp 1.1a	0.2	**0.3**	0.00	**2.3**	0.00	**1.0**	0.00	
	0.6	**1.2**	0.00	**16.0**	0.00	**5.3**	0.00	
Exp 1.1b	0.1	**0.2**	0.00	**2.7**	0.00	**0.9**	0.00	
	-1.2	**-2.3**	0.00	**-22.6**	0.00	**-8.6**	0.00	
Exp 1.1c	0.2	**0.4**	0.00	**4.7**	0.00	**1.7**	0.00	
	0.0	**0.1**	0.00	**0.6**	0.00	**0.2**	0.00	
Exp 1.2a	-0.3	**-0.5**	0.00	**-3.7**	0.00	**-1.6**	0.00	
	-0.8	**-1.5**	0.00	**-18.4**	0.00	**-6.2**	0.00	
	0.3	**0.6**	0.00	**4.5**	0.00	**1.9**	0.00	
	0.2	**0.3**	0.00	**2.7**	0.00	**1.0**	0.00	
Exp 1.2b	-0.4	**-0.7**	0.00	**-4.0**	0.00	**-1.9**	0.00	
	0.1	**0.2**	0.00	**1.7**	0.00	**0.7**	0.00	
	1.4	**2.6**	0.00	**38.5**	0.00	**12.1**	0.00	
	-0.7	**-1.3**	0.00	**-72.8**	0.00	**-12.5**	0.00	
	-0.3	**-0.6**	0.00	**-19.3**	0.00	**-4.2**	0.00	
	0.2	**0.4**	0.00	**0.0**	0.22	**0.0**	0.22	
Exp 2.1	-4.0	**-6.2**	0.00	**-14.7**	0.00	**-10.0**	0.00	
	-5.3	**-8.2**	0.00	**-19.9**	0.00	**-13.4**	0.00	
Exp 2.2	-5.2	**-7.6**	0.00	**-15.0**	0.00	**-11.0**	0.00	
	-6.1	**-9.1**	0.00	**-20.0**	0.00	**-14.1**	0.00	
Exp 2.3	2.5	**3.2**	0.00	**4.9**	0.00	**4.0**	0.00	
	3.0	**3.8**	0.00	**5.7**	0.00	**4.7**	0.00	
Exp 2.4	1.1	**1.6**	0.00	**3.4**	0.00	**2.4**	0.00	
	2.2	**2.9**	0.00	**4.8**	0.00	**3.8**	0.00	
Exp 2.5	2.8	**4.2**	0.00	**8.5**	0.00	**6.2**	0.00	
	12.2	**18.1**	0.00	**37.1**	0.00	**27.0**	0.00	
Exp 2.6	2.2	**3.8**	0.00	**20.9**	0.00	**10.2**	0.00	
	4.2	**6.8**	0.00	**19.1**	0.00	**12.2**	0.00	

Figures captions:

Figure 1. Oxygen isotope fractionation during denitrification as a result of branching effects (ε_{NAR}, ε_{NIR}, ε_{NOR}) und exchange effects (ε_w) associated with the following enzymatic reaction steps: NAR, NIR and NOR.

Figure 2. Correlation between oxygen isotopic signatures of N_2O and soil water expressed in relation to soil nitrate, the equation of linear fit allows for estimation of isotope exchange with soil water (slope of the linear fit) and the associated isotope effect (intercept of the linear fit). In red the influence of N_2O reduction on the method performance is presented - red X points represent the samples with not inhibited N_2O reduction (note that the slope and intercept are very different), whereas the red + points stand for the same samples after mathematical correction of N_2O reduction effect (as described in Sect. 2.5) which fit very well to the samples where N_2O reduction was inhibited. Data from Exp 1.

Figure 3. Relation between relative isotope ratio differences between produced N_2O and soil water ($\delta_0{}^{18}O(N_2O/H_2O)$ and between produced N_2O and soil nitrate ($\delta_0{}^{18}O(N_2O/NO_3^-)$, on the right $\delta^{18}O$ values of the initial soil nitrate for different treatments. $\delta^{18}O$ values of the initial soil water ranged between -13.5 and -1.6 ‰ (see Table 1) and its variation had no impact on $\delta_0{}^{18}O(N_2O/H_2O)$. Open symbols: treatments with synthetic nitrate as fertilizer, filled symbols: treatments with natural Chile saltpeter as fertilizer. Data from Exp 1.

Figure 4. $\delta_0{}^{18}O(N_2O/H_2O)$ as a function of isotope exchange extent, x (determined with $\Delta^{17}O$ method). Red symbols: Exp 1, black symbols: Exp 2; open symbols: incubations with lower WFPS (70 %), filled symbols: incubations with higher WFPS (80 %). Note that same symbols shapes always represent the same soil.

Figure 5. Relation between $\delta_0{}^{15}N^{sp}$ of produced N_2O and relative ratio difference between produced N_2O and soil water ($\delta_0{}^{18}O(N_2O/H_2O)$). Red symbols: Exp 1, black symbols: Exp 2; open symbols: incubations with lower WFPS (70 %), filled symbols: incubations with higher WFPS (80 %). Note that same symbols shapes always represent the same soil. Grey dashed lines represent the possible range of linear fit when extreme values of isotope effects for N_2O reduction are assumed in correction calculations (Eq. (5)). Range of values for fungal denitrification from Rohe et al. (2014a).

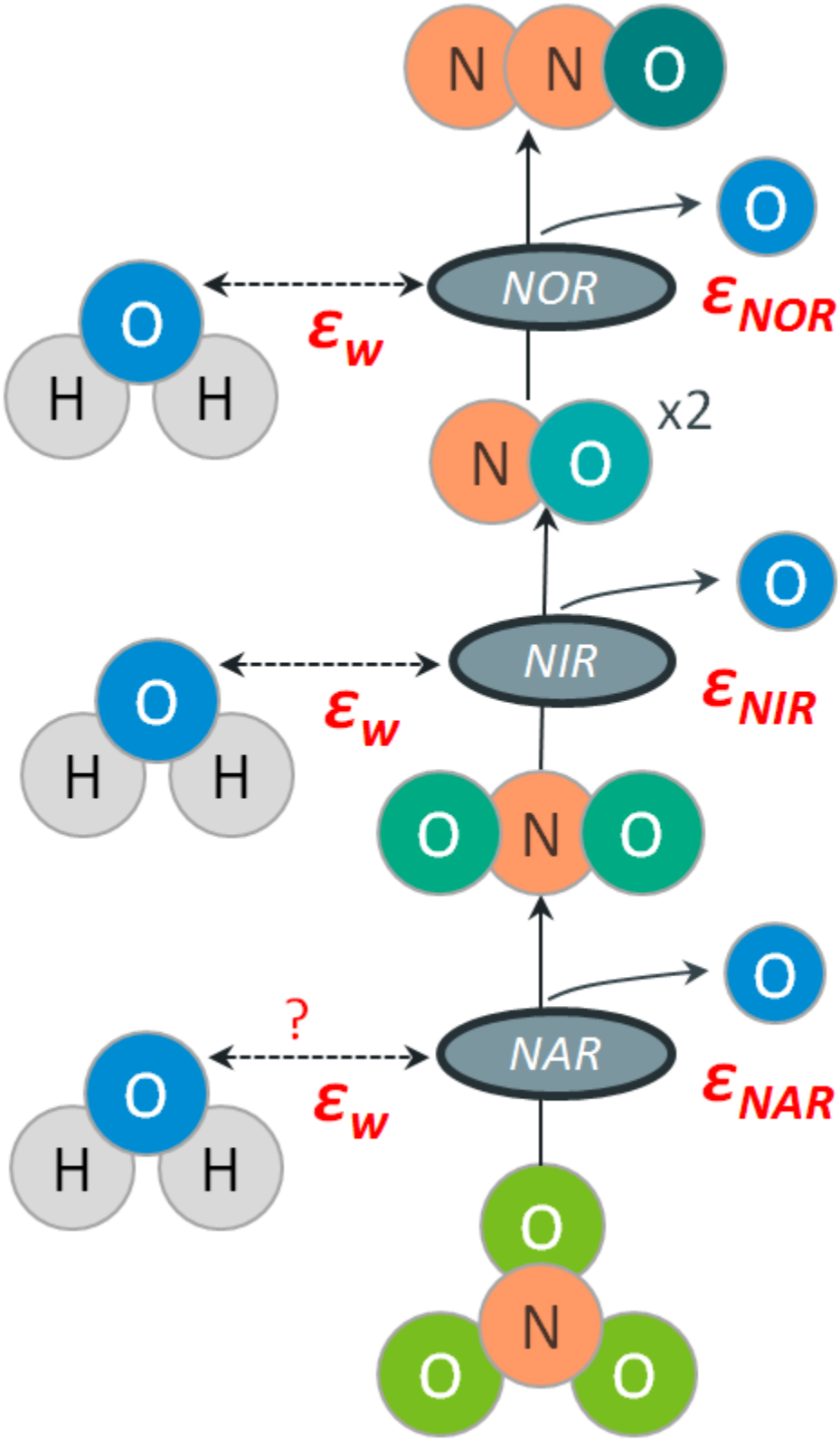
N N O
O
NOR
ε_{NOR}
O H H
ε_w
N O
x2
O
NIR
ε_{NIR}
O H H
ε_w
O N O
O
?
NAR
ε_{NAR}
O H H
ε_w
O
N
O O

Fig.1

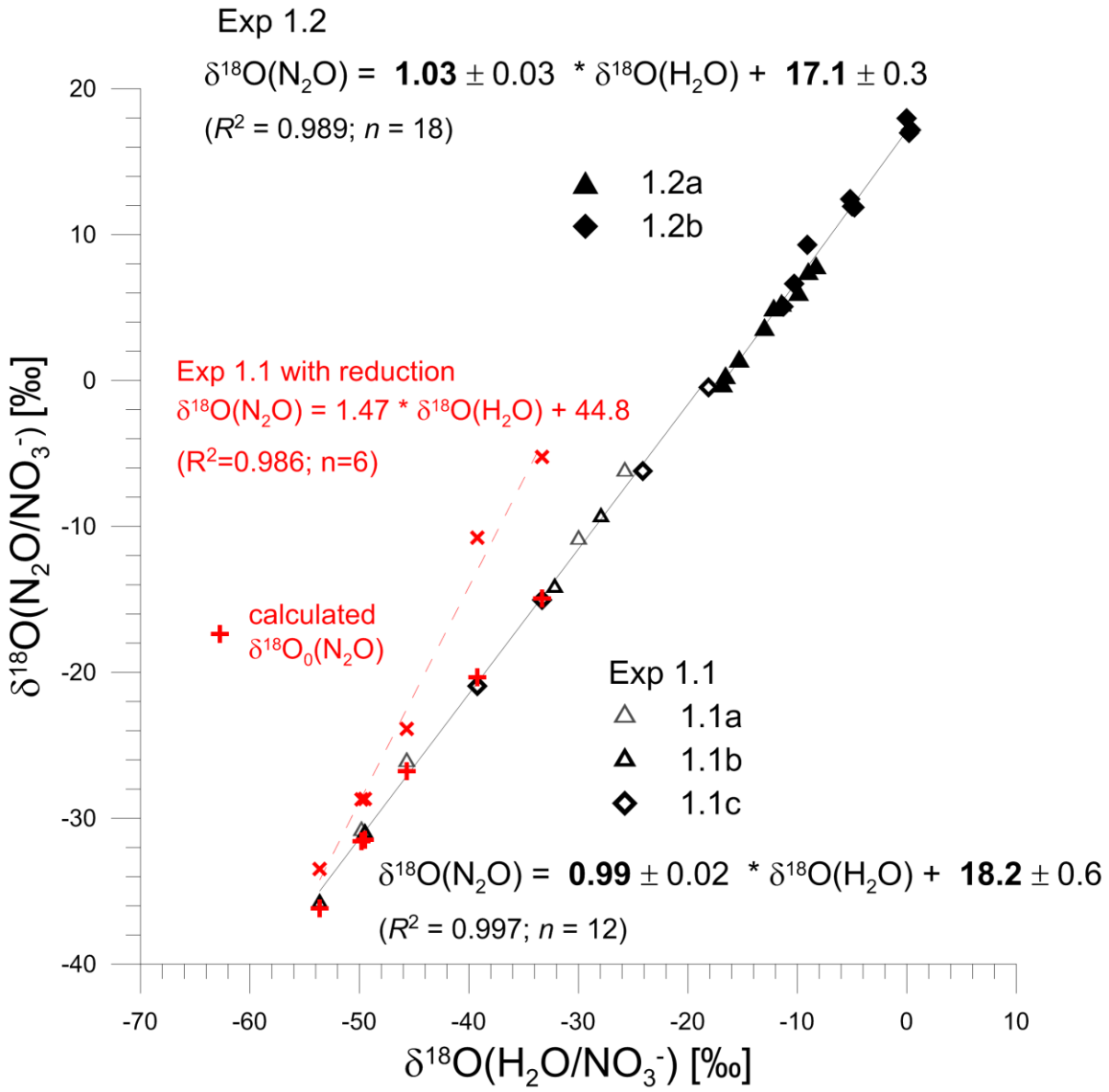
Exp 1.2
δ18O(N2O) = 1.03 ± 0.03 * δ18O(H2O) + 17.1 ± 0.3
(R2 = 0.989; n = 18)
1.2a
1.2b
Exp 1.1 with reduction
δ18O(N2O) = 1.47 * δ18O(H2O) + 44.8
(R2=0.986; n=6)
calculated
δ18O0(N2O)
Exp 1.1
1.1a
1.1b
1.1c
δ18O(N2O) = 0.99 ± 0.02 * δ18O(H2O) + 18.2 ± 0.6
(R2 = 0.997; n = 12)
δ18O(N2O/NO3-) [‰]
δ18O(H2O/NO3-) [‰]
20
10
0
-10
-20
-30
-40
-70
-60
-50
-40
-30
-20
-10
0
10

Fig.2

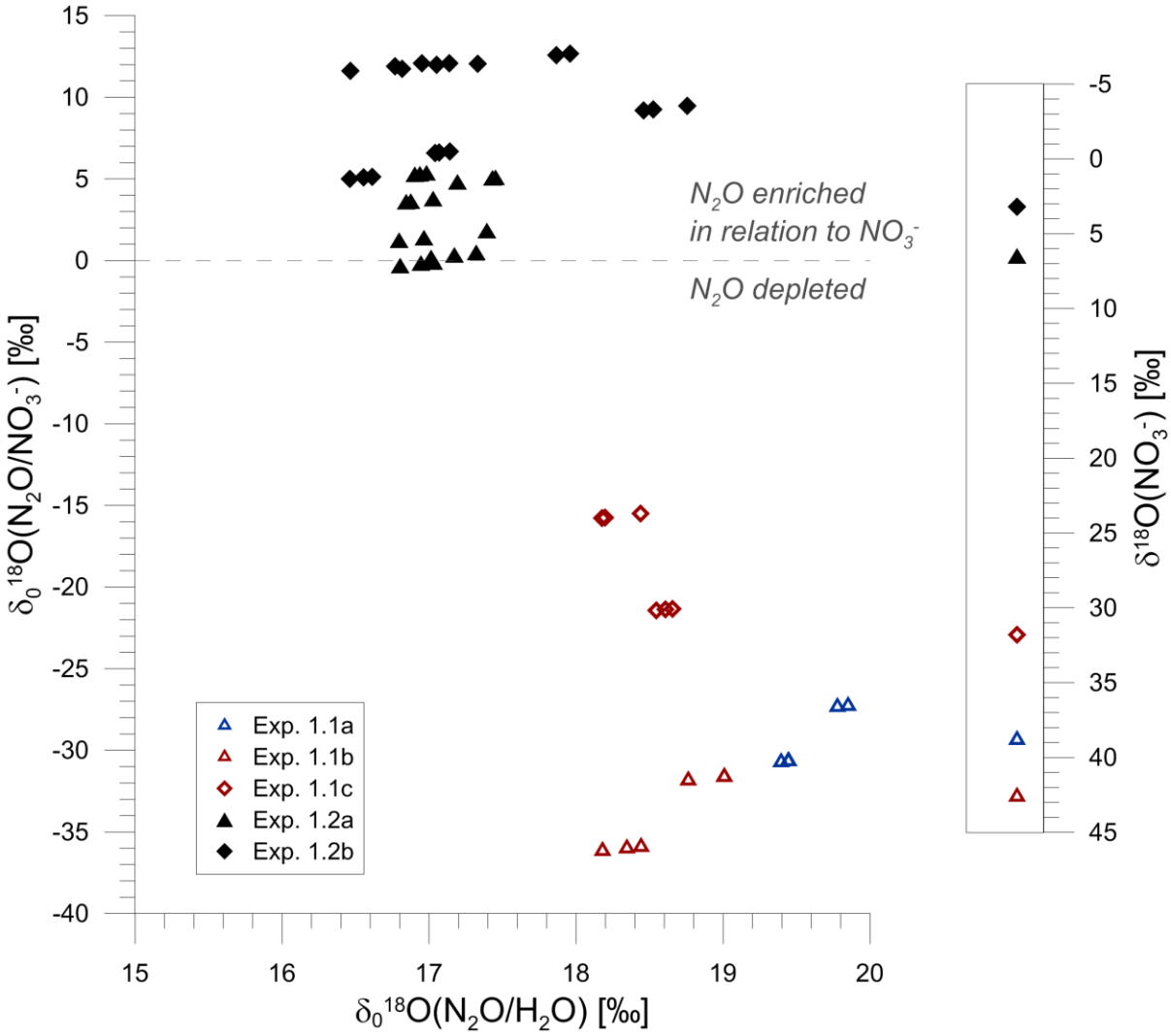
15
10
5
0
-5
-10
-15
-20
-25
-30
-35
-40
15
16
17
18
19
20
δ0 18O(N2O/H2O) [‰]
δ0 18O(N2O/NO3-) [‰]
N2O enriched
in relation to NO3-
N2O depleted
Exp. 1.1a
Exp. 1.1b
Exp. 1.1c
Exp. 1.2a
Exp. 1.2b
-5
0
5
10
15
20
25
30
35
40
45
δ18O(NO3-) [‰]

Fig.3

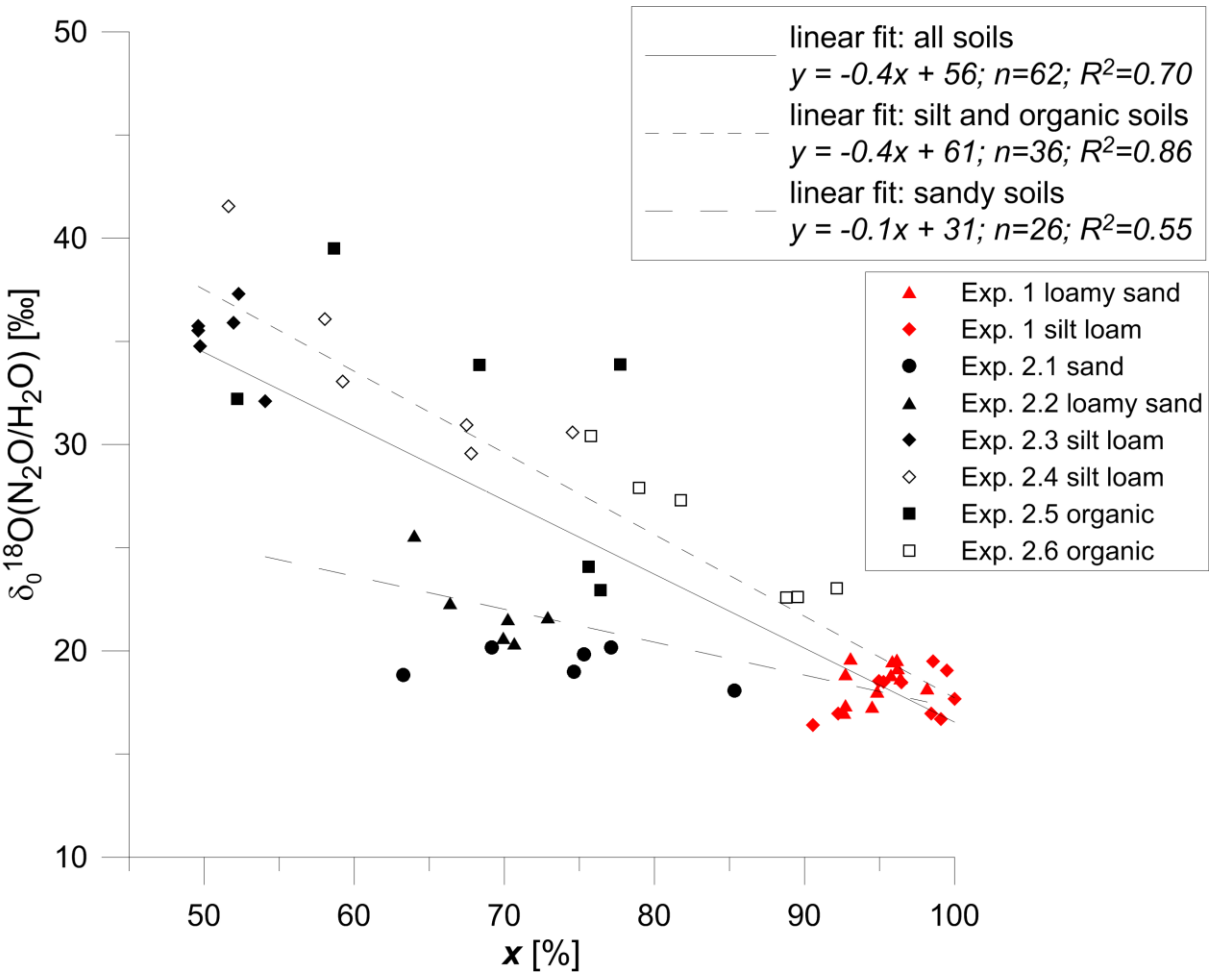
linear fit: all soils
y = -0.4x + 56; n=62; R2=0.70
linear fit: silt and organic soils
y = -0.4x + 61; n=36; R2=0.86
linear fit: sandy soils
y = -0.1x + 31; n=26; R2=0.55
Exp. 1 loamy sand
Exp. 1 silt loam
Exp. 2.1 sand
Exp. 2.2 loamy sand
Exp. 2.3 silt loam
Exp. 2.4 silt loam
Exp. 2.5 organic
Exp. 2.6 organic
δ0 18O(N2O/H2O) [‰]
x [%]
50
40
30
20
10
50
60
70
80
90
100

Fig.4

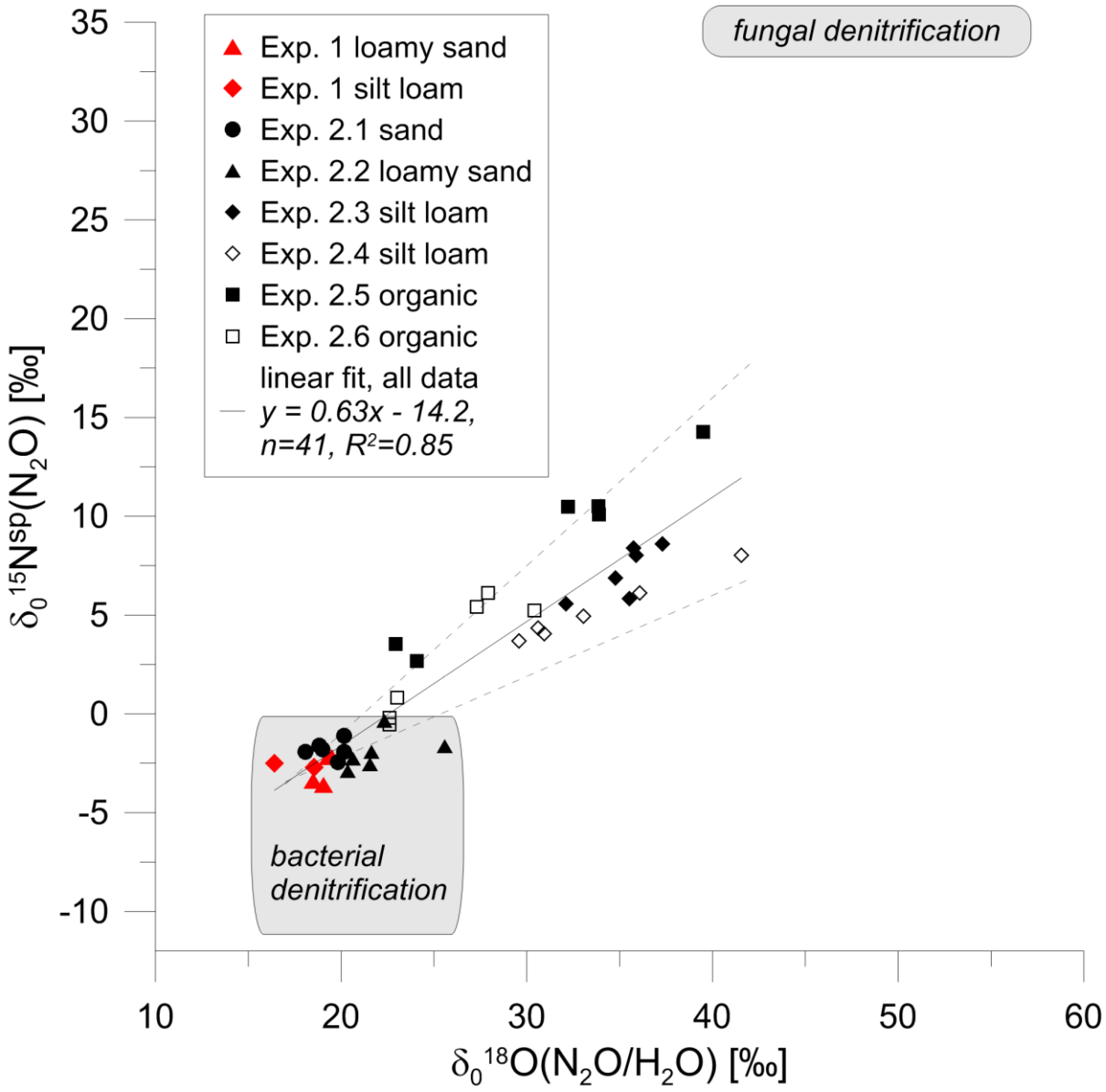
fungal denitrification
Exp. 1 loamy sand
Exp. 1 silt loam
Exp. 2.1 sand
Exp. 2.2 loamy sand
Exp. 2.3 silt loam
Exp. 2.4 silt loam
Exp. 2.5 organic
Exp. 2.6 organic
linear fit, all data
y = 0.63x - 14.2,
n=41, R²=0.85
bacterial denitrification
δ0 15Nsp(N2O) [‰]
δ0 18O(N2O/H2O) [‰]
35
30
25
20
15
10
5
0
-5
-10
10
20
30
40
50
60

Fig.5